~~SECRET~~

Unclassified

UMM-127 = RL-2017

Studies in Radar Cross-Sections - XII

Summary of Radar Cross-Section Studies under Project MIRO

by K. M. Siegel, M. E. Anderson, R. R. Bonkowski, and W. C. Orthwein

Project MIRO
Contract No. AF 30(602)-9

Willow Run Research Center
Engineering Research Institute
University of Michigan
UMM-127 December, 1953

Unclassified

~~SECRET~~

~~This document contains information affecting the national defense of the United States within the meaning of the Espionage Laws, Title 18, U.S.C., Sections 793 and 794. Its transmission or the revelation of its contents in any manner to an unauthorized person is prohibited by law.~~

See note inside

FOR INTRA-UNIVERSITY CORRESPONDENCE

UNIVERSITY OF MICHIGAN

ENGINEERING RESEARCH INSTITUTE

21 February 1958

MEMO TO: Prof. K. M. Siegel

FROM: Security Office

SUBJECT: Project 2015

This is to advise you that all reports and memos generated on Project 2015 (AF30(602)9 are unclassified.

Please see that all documents in your possession are marked in the manner illustrated below. Regrading markings should appear on front and back covers, title, first and last pages, with the previous classification lined through.

CLASSIFICATION
CHANGED TO
UNCLASSIFIED
AS PER AUTHORITY
chang order RADC
14 Aug 56 - R.B. McInerney

Bulk files of aforementioned reports need not be so marked immediately. Regrading markings can be affixed when the documents are being used or charged out or transmitted. However, if bulk files are in your possession, the change of classification should be indicated inside the file drawer or storage container.

Victor J. Scodius

V. J. SCODIUS
Security Officer

fg
c.c.: J. H. Richter

UMM 127

Studies in Radar Cross-Sections - XII: Summary of Radar Cross-Section Studies Under Project MIRO, by K. M. Siegel, M. E. Anderson, R. R. Bonkowski, and W. C. Orthwein (UMM-127, December 1953). Contract No. AF 30(602)-9. SECRET.

Errata

Pg. 47, 1st col., 6th row	Replace 4" sq. 1/8" thick) by 4" sq., 0.8" thick)
Pg. 53, Ref. A.10	Replace 308-23 by 302-23
Pg. 89, 4th col., 2nd row	Replace .12 by .02

Addenda

None

TABLE OF CONTENTS

LIST OF FIGURES

LIST OF TABLES

PREFACE

This paper is the twelfth in a series of reports growing out of studies of radar cross-sections at the University of Michigan's Willow Run Research Center. The primary aims of this program are:

(1) To show that radar cross-sections can be determined analytically.

(2) To elaborate means for computing cross-sections of objects of military interest.

(3) To demonstrate that these theoretical cross-sections are in agreement with experimentally determined values.

Intermediate objectives are:

(1) To compute the exact theoretical cross-sections of various simple bodies by solution of the appropriate boundary-value problems arising from the electromagnetic vector wave equation.

(2) To examine the various approximations possible in this problem, and determine the limits of their validity and utility.

(3) To find means of combining the simple body solutions in order to determine the cross-sections of composite bodies.

(4) To tabulate various formulas and functions necessary to enable such computations to be done quickly for arbitrary objects.

(5) To collect, summarize, and evaluate existing experimental data.

Titles of the papers already published or presently in process of publication are listed on the inside of the front cover.

K. M. Siegel

SUMMARY OF RADAR CROSS-SECTION STUDIES

The need for work in the radar cross-section field has been well expressed in a recent USAF report (Ref. 1), as follows:

"During World War II, many measurements of aircraft radar reflection characteristics were made but unfortunately almost none were made with sufficient accuracy and uniformity of measurement technique that they can be considered meaningful.

"As a result of these measurements, contractors and components of the Air Force are using values of echo area that vary in value and are insufficient in detail to allow proper calculations of factors vital in the research and development of radar equipment."

The Willow Run Research Center, because of its interest in parameters which are vital in Air Defense system problems, started an analysis of the radar cross-section field in 1949. It is believed that the capability now exists at the Willow Run Research Center to determine the radar cross-section of any target of military importance to within a factor of 10.

Radar cross-sections may be determined either theoretically or experimentally. In either case great difficulties are encountered. In the precise theoretical determination of cross-sections the mathematical complexity is so great that the analytical problem can be solved only for the simplest shapes, and even then the computational procedures in obtaining numerical answers are forbiddingly difficult. To date the analytical problem has been solved only for five shapes: sphere, prolate spheroid, oblate spheroid, semi-infinite cone, and semi-infinite paraboloid. However, approximations are known for a great many other shapes, including the following: finite cone, finite paraboloid, ogive, circular cylinder, elliptical cylinder, wire, thick dipole, wedge, circular disk, rectangular flat plate, various corners, hyperboloid of one sheet, hyperboloid of two sheets, and torus. Furthermore composite bodies composed of mixtures of these simple shapes are also subject to approximate analytic methods, which yield appropriate solutions. Finally, real objects, such as aircraft, may be approximated by composite groups of such simple shapes, again within the limits of the necessary accuracy of the approximation. These methods of approximation are discussed in some detail in other papers of this series, notably References 2 and 3.

The over-all results of any such approximation method should be accurate within a factor of 10. It is of course hoped that the approximations will be better in many cases, but this maximum error is tolerable because the range of detection varies as the fourth root of the cross-section. In other words, if the radar cross-section is known within a factor of 10, the range performance of the radar system is known within a factor of 1.78.

The other method of determining radar cross-sections is by experimental measurements. These measurements may be made on full-size objects or on scale models, and they may be either static or dynamic in nature. Many difficulties plague each of these types of experiments, and again it is difficult to be certain that answers obtained are reliable within a factor of 10. In static experiments the model or full-scale object must be suspended in some way away from the earth, and it is difficult to eliminate reflections from the supports. Furthermore there are likely to be reflections from the ground. It is often difficult to guarantee that the radar and the scatterer are sufficiently far apart so that the results can be truly said to represent a far-zone (as distinguished from a near-zone) cross-section. In dynamic experiments it is difficult to measure the exact aspect and range of the object at the instant the measurement is made, and furthermore calibration difficulties are frequently involved because of the difficulty of getting a comparison object at the same range within a reasonable time. In all cases there are difficulties in eliminating reflections from spurious targets in side lobes, and numerous other instrumentation difficulties. Measurement of cross-section of full sized objects presents obvious difficulties connected with the expense of the experiments, whereas the use of scale models brings into question the appropriate modeling theory and also leads to questions of the accuracy of the models.

For all of these reasons, a particular number which is produced as representing the cross-section of any particular object is not likely to be reliable unless this number has been verified both by several different types of experimental measurements and by theoretical calculations. The only cross-section values which could probably be relied on to within an accuracy of a few per cent are those of the simple shapes mentioned above for which exact electromagnetic solutions are available. In some cases, however, numerous static and dynamic experiments on both full-scale objects and scale models have given answers all in the same neighborhood, and when these answers are further corroborated by theoretical evidence there can be considerable confidence in the results, and also in the approximation technique used.

In general, then, an approximation method can be considered reliable and physically significant if it satisfies the following tests:

a) A collection of simple shapes (such as those listed above) can be substituted for the actual object in question (for example, an aircraft) without appreciably changing the scattering effect on electromagnetic radiation.

b) A suitable numerical solution is available for the resulting collection of simple shapes, which is a good approximation for the exact answer to this collection of simple shapes.

c) Some member of the class or kind of composite configuration (like fighters with swept-back fins) should have had its cross-section measured in a laboratory and the approximation method when applied to that configuration must have yielded results which were within a factor of 10 of the measured results averaged over some suitable range in angle (usually determined by expected accuracy of the experimental equipment).

Many of the approximation techniques which lead to the numerical results mentioned in Appendix B, and which will be analyzed in another paper of this series, have met all of these tests.

This report, the final radar cross-section report sponsored under Project MIRO, summarizes many parts of the radar cross-section field. In particular it brings up to date all knowledge available to us on the radar cross-section of aircraft and other airborne military vehicles (such as guided missiles). In Appendix A is presented an up-to-date summary of all known experimental values of radar cross-sections of aircraft, missiles, and artillery and mortar projectiles. This summary includes both dynamic and static measurements on both full-scale targets and on models. This table replaces the corresponding portions of the similar tabulation in Reference 4. In Appendix B are tabulated all of the theoretical values of radar cross-sections of aircraft and airborne missiles which have been computed by the Willow Run Research Center. (The corresponding theoretical calculations for ballistic missiles will be published separately later.) In three cases these theoretical results are compared with experimental results. In Appendix C are discussed all the exact values of radar cross-sections presently known for three-dimensional configurations.

The radar cross-section field, and the series of papers of which this is a part, must be viewed as a whole. It is of interest to note, for example, that the cross-section of a prolate spheroid which was analyzed at Willow Run Research Center under Project Wizard has been of value because the fuselage of many aircraft can be approximated by a prolate spheroid. Also the cross-section of a cone, which was analyzed under Project MIRO, has been of value because the cone (and the closely related configuration known as the ogive) are important in computing the cross-section of ballistic missiles. The work on the radar cross-section of the sphere has been applied to the scattering of light by air molecules, water droplets, and dust.

It appears that there is considerable utility in theoretical radar cross-section studies of the type which are reported in this series, and that the fundamental theoretical work has now proceeded to the point where a maximum of pay-off can be obtained with a minimum of effort. It is therefore recommended that this type of effort be maintained. In particular, it is recommended that continuing surveys be made of the theoretical work being done and the experimental results reported in the radar cross-section field, and that these results be tabulated and circulated periodically. It is also recommended that a continuing study be made of new and old methods of obtaining radar cross-sections of composite shapes (missiles and aircraft) to determine the best methods available for radar cross-section determinations. Finally it is recommended that such a group be maintained so that it is available to supply particular radar cross-section estimates in accordance with requests for such data from appropriate authorities in the Department of Defense.

REFERENCES
FOR THE TEXT

1. Wm. F. Bahret, "Dynamic Measurements of Aircraft Radar Reflection Characteristics, Part 1: Measurement Equipment and Techniques", Wright Air Development Center Technical Report 53-148 (April 1953) UNCLASSIFIED.

2. R. R. Bonkowski, C. R. Lubitz, and C. E. Schensted, "Studies In Radar Cross-Sections VI: Cross-Sections of Corner Reflectors and Other Multiple Scatterers at Microwave Frequencies", Willow Run Research Center, University of Michigan, External Report No. UMM-106 (October 1953) SECRET (UNCLASSIFIED when appendix is removed).

3. K. M. Siegel, H. A. Alperin, R. R. Bonkowski, J. W. Crispin, A. L. Maffett, C. E. Schensted, and I. V. Schensted, "Studies in Radar Cross-Sections VIII: Theoretical Cross-Sections as a Function of Separation Angle Between Transmitter and Receiver at Small Wavelengths", Willow Run Research Center, University of Michigan, External Report No. UMM-115 (October, 1953) UNCLASSIFIED.

4. K. M. Siegel, J. W. Crispin, and R. E. Kleinman, "Studies in Radar Cross-Sections VII: Summary of Radar Cross-Section Studies Under Project Wizard", Willow Run Research Center, University of Michigan, External Report No. UMM-108 (November, 1952) SECRET.

APPENDIX A

COMPENDIUM OF EXPERIMENTAL CROSS-SECTION DATA

The Willow Run Research Center has continued collecting and tabulating cross-section data. The results of this tabulation are presented in this appendix. For the sake of unity this present survey embraces all of the material previously presented [Ref. A1], with occasional corrections and the deletion of some retracted data. In addition, a considerable amount of new data is presented. These tables thus represent all published experimental data known* to the authors. However, it is to be stressed that the following tables are neither presumed nor intended to be exhaustive, but rather representative. Frequently, the data given for sample aspects is taken from a more complete tabulation or from entire polar diagrams of cross-section. Hence, the original references should be consulted if more specific and detailed information is desired.

Attention is called to the fact that a very exhaustive bibliography of research on radar reflections has appeared recently [Refs. A2, A3, A4]. This bibliography contains abstracts and comments on over 1000 published articles. While very little numerical cross-section data is included, these three volumes are an invaluable reference and catalog aid to researchers in this field.

*If the reader knows of any data not covered herein, the authors would appreciate obtaining references to them.

Table A-1: Missile Cross-Sections

Body	Equipment	Polarization	Static or Dynamic	Frequency (in mc/s)	CW or Pulse	Aspect	Radar Cross-Section (in m^2)	Ref
Corporal E (model)	Hybrid T	Horizontal	Static	20	CW	Nose-on Broadside Tail-on	0.78 79 < 0.09	A5
"	"	Vertical	"	50	"	Nose-on Broadside Tail-on	23 26 25	A6
"	"	Horizontal	"	100	"	Nose-on Broadside Tail-on	1.5 133 2.7	A7
"	"	Vertical	"	300	"	Nose-on Broadside Tail-on	3.6 137 2.2	A8
"	"	Horizontal	"	600	"	Nose-on Broadside Tail-on	0.35 137 7	A9
"	"	Vertical	"	600	"	Nose-on Broadside Tail-on	0.61 91 8.6	A9
"	"	Horizontal	"	1200	"	Nose-on Broadside Tail-on	0.012 16 3.3	A10
"	"	Vertical	"	1200	"	Nose-on Broadside Tail-on	0.012 11 2.4	A10
Hermes A (model)	Underwater Sound Method	--	--	1666	--	Nose-on	0.0078	A11

Table A-1: Missile Cross-Sections (Cont.)

Body	Equipment	Polarization	Static or Dynamic	Frequency (in mc/s)	CW or Pulse	Aspect	Radar Cross-Section (in m^2)	Ref
Nike (model)	Underwater Sound Method	--	Static	Equivalent to x-band	--	Nose-on	0.064	A11
"	"	--	"	Equivalent to k-band	--	Nose-on	0.013	A11
Rocket model (without fins) length = 3.8 λ diameter = 0.6 λ 30^o ogive nose	Hybrid T	Perpendicular to axis of rotation	"	9375	CW	Nose-on	8.2	A12
Rocket model (with fins) length = 3.8 λ diameter = 0.6 λ 30^o ogive nose	"	"	"	9375	"	Nose-on	0.2	A12
UMA-1 with fins (model)	"	Horizontal	"	568	"	Nose-on	1.25	A13
"	"	Vertical	"	568	"	Nose-on	0.56	A13
UMA-1 without fins (model)	"	Horizontal	"	568	"	Nose-on	0.45	A13

Table A-1: Missile Cross-Sections (Cont.)

Body	Equipment	Polarization	Static or Dynamic	Frequency (in mc/s)	CW or Pulse	Aspect	Radar Cross-Section (in m^2)	Ref
UMA-1 without fins (model)	Hybrid T	Vertical	Static	568	CW	Nose-on	0.45	A13
V-2 (model)	"	Horizontal	"	20	"	Nose-on Broadside Tail-on	9.7 128 6.5	A14
"	"	Vertical	"	20	"	Nose-on Broadside Tail-on	6.6 30 8.5	A14
"	"	Horizontal	"	50	"	Nose-on Broadside Tail-on	29 200 17	A14
"	"	Vertical	"	50	"	Nose-on Broadside Tail-on	25 241 14	A14
"	AN/TPQ-2	Horizontal	"	50	Pulse	Nose-on	30	A15
"	"	Vertical	"	50	"	Nose-on	25	A15
"	Hybrid T	Horizontal	"	100	CW	Nose-on Broadside Tail-on	3.3 400 5.7	A7
"	AN/TPQ-2	"	"	100	Pulse	Nose-on	11	A15

Table A-1: Missile Cross-Sections (Cont.)

Body	Equipment	Polarization	Static or Dynamic	Frequency (in mc/s)	CW or Pulse	Aspect	Radar Cross-Section (in m^2)	Ref
V-2 (model)	AN/TPQ-2	Vertical	Static	100	Pulse	Nose-on	6	A15
V-2	SCR-270	--	Dynamic	109	"	--	Peak radar area 147 (before fuel cut-off), 0.3 - 3 (after fuel cut-off)	A16
V-2 (model)	AN/TPQ-2	Horizontal	Static	110	"	Nose-on	9	A15
"	"	Vertical	"	110	"	Nose-on	6.5	A15
"	"	Horizontal	"	200	"	Nose-on	2.8	A15
"	"	Vertical	"	200	"	Nose-on	2	A15
"	"	Horizontal	"	250	"	Nose-on	2	A15
"	"	Vertical	"	250	"	Nose-on	0.85	A15

Table A-1: Missile Cross-Sections (Cont.)

Body	Equipment	Polarization	Static or Dynamic	Frequency (in mc/s)	CW or Pulse	Aspect	Radar Cross-Section (in m^2)	Ref
V-2 (model)	AN/TPQ-2	Horizontal	Static	300	Pulse	Nose-on	0.46	A15
"	"	Vertical	"	300	"	Nose-on	1	A15
"	Hybrid T	Horizontal	"	300	CW	Nose-on Broadside Tail-on	7.4 73 14	A8
"	AN/TPQ-2	"	"	500	Pulse	30° off nose 60° off nose	2.5 0.26	A15
"	"	"	"	500	"	Nose-on Broadside Tail-on	1.3 197 3.2	A15
"	"	Vertical	"	500	"	Nose-on	0.5	A15
"	Hybrid T	Horizontal	"	600	CW	Nose-on Broadside Tail-on	2.6 166 73	A9
"	"	"	"	600	"	30° off nose 60° off nose	0.61 0.97	A9
"	AN/TPQ-2	"	"	750	Pulse	Nose-on Broadside Tail-on	0.19 994 5.1	A15

Table A-1: Missile Cross-Sections (Cont.)

Body	Equipment	Polarization	Static or Dynamic	Frequency (in mc/s)	CW or Pulse	Aspect	Radar Cross-Section (in m^2)	Ref
V-2 (model)	AN/TPQ-2	Horizontal	Static	750	Pulse	30° off nose 60° off nose	0.19 0.5	A15
"	"	Vertical	"	750	"	Nose-on Broadside Tail-on	0.24 994 11	A15
"	"	"	"	750	"	30° off nose 60° off nose	1.1 1	A15
"	"	Horizontal	"	1000	"	Nose-on Broadside Tail-on	0.12 4780 56	A15
"	"	"	"	1000	"	30° off nose 60° off nose	0.5 4	A15
"	"	Vertical	"	1000	"	Nose-on Broadside Tail-on	0.18 650 26	A15
"	"	"	"	1000	"	30° off nose 60° off nose	0.49 2.6	A15
"	Hybrid T	Horizontal	"	1200	CW	Nose-on Broadside Tail-on	0.27 35 47	A10
"	"	"	"	1200	"	30° off nose 60° off nose	0.27 0.14	A10

Table A-1: Missile Cross-Sections (Cont.)

Body	Equipment	Polarization	Static or Dynamic	Frequency (in mc/s)	CW or Pulse	Aspect	Radar Cross-Section (in m^2)	Ref
V-2 (model)	Hybrid T	Vertical	Static	1200	CW	Nose-on Broadside Tail-on	0.11 30 30	A10
"	"	"	"	1200	"	30^{o} off nose 60^{o} off nose	0.11 0.14	A10
V-2	Radar (type unknown)	--	Dynamic	1250	Pulse	Various aspects	1	A17
"	"	--	"	3000	"	Tail-on	10-300	A17
"	AN/MPS-3	--	--	--	--	Nose-on Broadside	< 0.01 16	A18
"	"	--	--	--	--	30^{o} off nose 60^{o} off nose	0.09 0.3	A18
V-2 (model)	Bistatic radar (45^{o} between trans. and rec.)	Horizontal	Static	20	CW	Rec. nose-on Trans. nose-on	0.23 6.6	A19
"	"	Vertical	"	20	"	Rec. nose-on Trans. nose-on	4.9 4.2	A19
"	"	Horizontal	"	50	"	Rec. nose-on Trans. nose-on	2.8 3.3	A19

Table A-1: Missile Cross-Sections (Cont.)

Body	Equipment	Polarization	Static or Dynamic	Frequency (in mc/s)	CW or Pulse	Aspect	Radar Cross-Section (in m^2)	Ref
V-2 (model)	Bistatic radar (45^o between trans. and rec.)	Vertical	Static	50	CW	Rec. nose-on Trans. nose-on	15 12	A19
"	"	Horizontal	"	100	"	Rec. nose-on Trans. nose-on	0.11 0.19	A19
"	"	Vertical	"	100	"	Rec. nose-on Trans. nose-on	0.038 0.061	A19
"	Bistatic radar (30^o between trans. and rec.)	Horizontal	"	300	"	Rec. nose-on Trans. nose-on	2.2 2	A19
"	"	Vertical	"	300	"	Rec. nose-on Trans. nose-on	2 1.6	A19
"	"	Horizontal	"	600	"	Rec. nose-on Trans. nose-on	0.77 0.97	A19
"	"	Vertical	"	600	"	Rec. nose-on Trans. nose-on	0.47 0.14	A19
WAC (model)	Hybrid T	Horizontal	"	20	"	Nose-on Broadside Tail-on	0.002 32 < 0.04	A5
"	"	"	"	50	"	Nose-on Broadside Tail-on	0.19 13 0.27	A6

Table A-1: Missile Cross-Sections (Cont.)

Body	Equipment	Polarization	Static or Dynamic	Frequency (in mc/s)	CW or Pulse	Aspect	Radar Cross-Section (in m^2)	Ref
WAC (model)	Hybrid T	Horizontal	Static	100	CW	Nose-on Broadside Tail-on	3.6 16 4.9	A7
"	"	"	"	300	"	Nose-on Broadside Tail-on	0.53 22 0.41	A8
"	"	"	"	600	"	Nose-on Broadside Tail-on	0.18 19 2.5	A9
"	"	Vertical	"	600	"	Nose-on Broadside Tail-on	0.19 20 1.2	A9
"	"	Horizontal	"	1200	"	Nose-on Broadside Tail-on	0.35 20 0.8	A10
"	"	Vertical	"	1200	"	Nose-on Broadside Tail-on	0.2 20 0.74	A10
"	"	Horizontal	"	2900	"	Nose-on Broadside Tail-on	0.093 24 1.8	A20
"	"	Vertical	"	2900	"	Nose-on Broadside Tail-on	0.0058 6.4 1.3	A20

Table A-1: Missile Cross-Sections (Cont.)

Body	Equipment	Polarization	Static or Dynamic	Frequency (in mc/s)	CW or Pulse	Aspect	Radar Cross-Section (in m^2)	Ref
WAC (model)	Bistatic radar (30^o between trans. and rec.)	Horizontal	Static	1200	CW	Rec. nose-on Trans. nose-on	0.012 0.008	A19
"	"	Vertical	"	1200	"	Rec. nose-on Trans. nose-on	0.1 0.1	A19
"	"	Horizontal	"	2900	"	Rec. nose-on Trans. nose-on	0.093 0.061	A19
"	"	Vertical	"	2900	"	Rec. nose-on Trans. nose-on	0.048 0.048	A19

Table A-2: Shell Cross-Sections

Body	Equipment	Polarization	Static or Dynamic	Frequency (in mc/s)	CW or Pulse	Aspect	Radar Cross-Section (in m^2)	Ref
4.7" AA Shell	Doppler radar	Vertical	Static Doppler	23,700	--	Nose-on	0.009	A21
40 mm Bofor (model)	Hybrid T	"	Static	1200	CW	Nose-on	0.00002	A22
"	"	Horizontal	"	24,000	"	Nose-on Broadside Tail-on	0.0022 0.025 0.0079	A20
"	"	Vertical	"	24,000	"	Nose-on Broadside Tail-on	0.0012 0.025 0.007	A20
60 cal. (model)	"	Horizontal	"	1200	"	Nose-on	0.000061	A22
"	"	"	"	24,000	"	Nose-on Broadside Tail-on	0.000017 0.00074 0.00021	A20
"	"	Vertical	"	24,000	"	Nose-on Broadside Tail-on	0.000021 0.00052 0.00026	A20
60 mm Mortar Shell (model)	"	Horizontal	"	200	"	Nose-on Broadside Tail-on	0.00097 0.0035 0.00085	A23
"	"	Vertical	"	200	"	Nose-on Broadside Tail-on	0.00059 0.00051 0.00051	A23

Table A-2: Shell Cross-Sections (Cont.)

Body	Equipment	Polarization	Static or Dynamic	Frequency (in mc/s)	CW or Pulse	Aspect	Radar Cross-Section (in m^2)	Ref
60 mm Mortar Shell (model)	Hybrid T	Horizontal	Static	600	CW	Broadside	0.19	A24
"	"	Vertical	"	600	"	Broadside Tail-on	0.0034 0.0019	A24
"	"	Horizontal	"	1200	"	Nose-on	0.01	A25
"	"	"	"	2900	"	Nose-on	0.0002	A26
"	"	Vertical	"	2900	"	Nose-on	0.00093	A26
"	"	"	"	9000	"	Nose-on	0.017	A27
"	"	Horizontal	"	16,000	"	Nose-on Broadside Tail-on	0.0097 0.092 0.012	A28
"	"	Vertical	"	16,000	"	Nose-on Broadside Tail-on	0.018 0.092 0.015	A28
"	Doppler radar	"	Static Doppler	23,700	--	Nose-on	0.0024	A21

Table A-2: Shell Cross-Sections (Cont.)

Body	Equipment	Polarization	Static or Dynamic	Frequency (in mc/s)	CW or Pulse	Aspect	Radar Cross-Section (in m^2)	Ref
60 mm Mortar Shell (model)	Hybrid T	Horizontal	Static	24,000	CW	Nose-on Broadside Tail-on	0.029 0.13 0.015	A29
"	"	Vertical	"	24,000	"	Nose-on Broadside Tail-on	0.0038 0.034 0.012	A29
81 mm (large) Mortar Shell (model)	"	Horizontal	"	200	"	Broadside Tail-on	1.4 0.018	A23
"	"	Vertical	"	200	"	Nose-on Broadside Tail-on	0.00065 0.0079 0.0021	A23
81 mm (small) Mortar Shell (model)	"	Horizontal	"	200	"	Broadside	0.016	A23
"	"	Vertical	"	200	"	Nose-on Broadside Tail-on	0.0013 0.0026 0.0021	A23
81 mm (large) Mortar Shell (model)	"	Horizontal	"	600	"	Broadside	0.21	A24
"	"	Vertical	"	600	"	Nose-on Broadside Tail-on	< 0.005 0.056 < 0.02	A24
81 mm (small) Mortar Shell (model)	"	Horizontal	"	600	"	Broadside Tail-on	0.13 0.0035	A24

Table A-2: Shell Cross-Sections (Cont.)

Body	Equipment	Polarization	Static or Dynamic	Frequency (in mc/s)	CW or Pulse	Aspect	Radar Cross-Section (in m^2)	Ref
81 mm (small) Mortar Shell (model)	Hybrid T	Vertical	Static	600	CW	Nose-on Broadside Tail-on	0.049 0.22 0.041	A24
81 mm (large) Mortar Shell (model)	"	"	"	1200	"	Nose-on	0.038	A25
81 mm (small) Mortar Shell (model)	"	Horizontal	"	1200	"	Nose-on	0.012	A25
"	Doppler radar	Vertical	Static Doppler	2894	--	Nose-on	0.0025	A21
"	"	"	"	2894	--	Nose-on	0.00004	A21
81 mm (large) Mortar Shell (model)	Hybrid T	Horizontal	Static	2900	CW	Nose-on	0.012	A26
"	"	Vertical	"	2900	"	Nose-on	0.0093	A26
81 mm (medium) Mortar Shell (model)	"	Vertical	"	2900	"	Nose-on Broadside Tail-on	0.065 0.09 0.06	A30
81 mm (small) Mortar Shell (model)	"	Horizontal	"	2900	"	Nose-on	0.018	A26

Table A-2: Shell Cross-Sections (Cont.)

Body	Equipment	Polarization	Static or Dynamic	Frequency (in mc/s)	CW or Pulse	Aspect	Radar Cross-Section (in m^2)	Ref
81 mm (small) Mortar Shell (model)	Hybrid T	Vertical	Static	2900	CW	Nose-on	0.018	A26
81 mm (large) Mortar Shell (model)	"	"	"	9000	"	Nose-on	0.0049	A27
81 mm (small) Mortar Shell (model)	"	"	"	9000	"	Nose-on	0.0068	A27
81 mm Mortar Shell (model)	"	Horizontal	"	16,000	"	Nose-on Broadside Tail-on	0.016 0.11 0.046	A28
"	"	Vertical	"	16,000	"	Nose-on Broadside Tail-on	0.012 0.06 0.031	A28
81 mm (heavy) Mortar Shell (model)	"	Horizontal	"	16,000	"	Nose-on Broadside Tail-on	0.015 0.47 0.038	A28
"	"	Vertical	"	16,000	"	Nose-on Broadside Tail-on	0.025 0.432 0.064	A28
81 mm (large) Mortar Shell (model)	Doppler Radar	"	Static Doppler	23,700	--	Nose-on	0.0064	A21
81 mm (small) Mortar Shell (model)	"	"	"	23,700	--	Nose-on	0.0071	A21

Table A-2: Shell Cross-Sections (Cont.)

Body	Equipment	Polarization	Static or Dynamic	Frequency (in mc/s)	CW or Pulse	Aspect	Radar Cross-Section (in m^2)	Ref
81 mm (large) Mortar Shell (model)	Hybrid T	Horizontal	Static	24,000	CW	Nose-on Broadside Tail-on	0.0091 0.24 0.027	A29
"	"	Vertical	"	24,000	"	Nose-on Broadside Tail-on	0.0079 0.16 0.022	A29
81 mm (medium) Mortar Shell (model)	"	Horizontal	"	24,000	"	Nose-on Broadside Tail-on	0.0029 0.23 0.089	A29
"	"	Vertical	"	24,000	"	Nose-on Broadside Tail-on	0.016 0.04 0.12	A29
4.2" Mortar Shell without fins (model)	"	Horizontal	"	16,000	"	Nose-on Broadside Tail-on	0.017 0.47 0.075	A28
"	"	Vertical	"	16,000	"	Nose-on Broadside Tail-on	0.017 0.36 0.053	A28
Rifle Shells 5", 6", 8", 12", 18".	Radar (type unknown)	Horizontal	Dynamic	S, L, X-bands	--	18^o - 40^o off nose	At S and L-bands $2 \times 10^{-5} > \sigma > 2 \times 10^{-4}$ no return at X-band	A31
40 mm Shell	Doppler Radar	Vertical	Static Doppler	23,700	--	Nose-on	0.012	A21
90 mm Shell (model)	Hybrid T	Horizontal	Static	1200	CW	Nose-on	0.0056	A22

Table A-2: Shell Cross-Sections (Cont.)

Body	Equipment	Polarization	Static or Dynamic	Frequency (in mc/s)	CW or Pulse	Aspect	Radar Cross-Section (in m^2)	Ref
90 mm Shell (model)	Hybrid T	Vertical	Static	1200	CW	Nose-on	0.0056	A22
"	Doppler Radar	"	Static Doppler	23,700	--	Nose-on	0.008	A21
105 mm Shell (model)	Hybrid T	Horizontal	Static	1200	CW	Nose-on	0.0195	A22
120 mm Shell (model)	"	Vertical	"	1200	"	Nose-on	0.022	A22
"	"	"	"	1200	"	Tail-on (nose up 15°)	0.093	A22
155 mm Shell (model)	"	Horizontal	"	1200	"	Nose-on	0.028	A22
"	Doppler Radar	Vertical	Static Doppler	2894	--	Nose-on	0.00025	A21
"	Hybrid T	"	Static	2900	CW	Nose-on Broadside Tail-on	0.0038 0.27 0.16	A30
"	Doppler Radar	--	Static Doppler	9883	--	Nose-on	0.0027	A21

Table A-2: Shell Cross-Sections (Cont.)

Body	Equipment	Polarization	Static or Dynamic	Frequency (in mc/s)	CW or Pulse	Aspect	Radar Cross-Section (in m^2)	Ref
155 mm Shell (model)	Doppler Radar	Vertical	Static Doppler	23,700	--	Nose-on	0.057	A21
240 mm Shell (model)	"	--	"	9883	--	Nose-on	0.0096	A21
240 mm Shell	"	Vertical	"	23,700	--	Nose-on	0.0064	A21

Table A-3: Aircraft Cross-Sections

Body	Equipment	Polarization	Static or Dynamic	Frequency (in mc/s)	CW or Pulse	Aspect	Radar Cross-Section (in m^2)	Ref
Aircraft (fighters and bombers, including jets)	Modified CH Radar	--	Dynamic	22.7	--	--	2 - 80	A32
A-20	APG-16	Circular	"	X-band	--	Nose-on (approx) Broadside (approx)	4.4 5.2 (mean)	A33
"	"	Horizontal	"	"	--	Nose-on (approx) Broadside (approx) Tail-on (approx)	7.2 (mean) 86 (mean) 2.4 (mean)	A33
"	"	Vertical	"	"	--	Nose-on (approx)	8	A33
AT-11	Radar (type unknown)	--	"	--	--	All*	19	A34
"	--	--	"	--	--	Approaching and Receding	11	A35, A36
B-17 (model)	Hybrid T	Horizontal	Static	100	CW	Nose-on	9.3	A37
"	--	"	"	100	--	Nose-on Broadside Tail-on	115 740 16	A38
"	--	Vertical	"	100	--	Nose-on Broadside Tail-on	5 180 7	A38

*"All" indicates an average over several aspects.

Table A-3: Aircraft Cross-Sections (Cont.)

Body	Equipment	Polarization	Static or Dynamic	Frequency (in mc/s)	CW or Pulse	Aspect	Radar Cross-Section (in m^2)	Ref
B-17 (model)	Hybrid T	Horizontal	Static	450	CW	Approaching Receding	70 9.3	A36, A39
"	"	Vertical	"	450	"	Approaching Receding	8.5 6.1	A36, A39
"	--	Horizontal	"	450	--	Approaching Receding	23 12	A36, A40
"	--	Vertical	"	450	--	Approaching Receding	16 8	A36, A40
B-17	APG-33	--	Dynamic	--	Pulse	Tail-on	176	A41
"	Radar (type unknown)	--	"	--	--	All	74	A34
"	--	--	"	--	--	Approaching and Receding	45	A35, A36
B-18	--	--	"	--	--	Approaching and Receding	36	A35, A36
"	Radar (type unknown)	--	"	--	--	All	60	A34

Table A-3: Aircraft Cross-Sections (Cont.)

Body	Equipment	Polarization	Static or Dynamic	Frequency (in mc/s)	CW or Pulse	Aspect	Radar Cross-Section (in m^2)	Ref
B-18	Advanced Development System D2-1	--	Dynamic	10,000	--	All	65 (av)	A42
"	Advanced Development System J1-1	--	"	3000	--	All	65 (av)	A43
B-24 (model)	Hybrid T	Horizontal	Static	100	CW	Nose-on	93	A44
"	--	"	"	100	--	Nose-on Broadside Tail-on	50 1000 30	A38
"	--	Vertical	"	100	--	Nose-on Broadside Tail-on	40 800 20	A38
"	--	Horizontal	"	450	--	Approaching Receding	150 3	A36, A40
"	--	Vertical	"	450	--	Approaching Receding	20 5	A36, A40
B-24	Radar (type unknown)	--	Dynamic	--	--	All	60 (av)	A34
B-25	APG-33	--	"	--	Pulse	Nose-on Broadside Tail-on	22 46 5.7	A41

Table A-3: Aircraft Cross-Sections (Cont.)

Body	Equipment	Polarization	Static or Dynamic	Frequency (in mc/s)	CW or Pulse	Aspect	Radar Cross-Section (in m^2)	Ref
B-25	APG-36	--	Dynamic	--	Pulse	Nose-on Tail-on	93 ± 28 10.2 ± 4.6	A41
"	Radar (type unknown)	--	"	--	--	All	30 (av)	A34
"	TS-35A*	--	"	--	Pulse	--	9.6	A45
B-29	APG-36	--	"	--	"	Front	59 - 69	A41
"	"	--	"	--	"	Tail-on	69 ± 22	A41
"	TPS-1B	Horizontal	"	1250	"	Az. 12° - 27° Elev. 2° - 10°	80	A46
"	"	"	"	1250	"	Az. 5° - 7° Elev. 1° - 3°	10	A46
"	"	--	"	1250	"	All	103	A47
"	SP-1M	Horizontal	"	2810	"	Az. 12° - 27° Elev. 2° - 10°	250	A46

*Actually consisted of the TS-35A test set (used both as a power meter and a signal generator), antenna, directional coupler, waveguide, receiver, and "A" scope.

Table A-3: Aircraft Cross-Sections (Cont.)

Body	Equipment	Polarization	Static or Dynamic	Frequency (in mc/s)	CW or Pulse	Aspect	Radar Cross-Section (in m^2)	Ref
B-29	SP-1M	--	Dynamic	2810	Pulse	All	370	A47
"	MK-33	--	"	9380	"	All	75	A47
"	--	--	"	--	--	Approaching and Receding	67	A35, A36
B-36 (model)	Hybrid T	Horizontal	Static	73	CW	Nose-on Broadside Tail-on	3.4 2600 86	A48
"	"	Vertical	"	73	"	Nose-on Broadside Tail-on	1.7 1700 1.9	A48
B-36	TPS-1B	Horizontal	Dynamic	1250	Pulse	All	21 (mean)	A49
"	"	"	"	1250	"	Az. 359° Elev. $4^\circ - 10^\circ$	6.3	A50
"	SP-1M	"	"	2810	"	All	44 (mean)	A49
"	"	"	"	2810	"	Az. $31^\circ - 56^\circ$ Elev. $4^\circ - 6^\circ$	25	A50

Table A-3: Aircraft Cross-Sections (Cont.)

Body	Equipment	Polarization	Static or Dynamic	Frequency (in mc/s)	CW or Pulse	Aspect	Radar Cross-Section (in m^2)	Ref
B-36	MK-33	Horizontal	Dynamic	9380	Pulse	All	8.75	A49, A51
"	"	"	"	9380	"	Az. 359° Elev. 4° - 10°	4.5	A49, A51
B-45	TPS-1B	"	"	1250	"	Az. 11° Elev. 2° - 8°	6	A50
"	"	"	"	1250	"	All	>31	A52
"	"	"	"	1250	"	All (except Az. 85° - 95°)	12	A52
"	SP-1M	"	"	2810	"	Az. 11° Elev. 2° - 8°	14	A50
"	"	"	"	2810	"	All	28	A52
"	"	"	"	2810	"	All (except Az. 85° - 95°	11	A52
"	MK-33	"	"	9380	"	All	53	A52

Table A-3: Aircraft Cross-Sections (Cont.)

Body	Equipment	Polarization	Static or Dynamic	Frequency (in mc/s)	CW or Pulse	Aspect	Radar Cross-Section (in m^2)	Ref
B-45	MK-33	Horizontal	Dynamic	9380	Pulse	All (except Az. 85° - 95°)	11	A52
B-47 (model)	Hybrid T	"	Static	73	CW	Nose-on Broadside Tail-on	11 780 2	A53
"	"	Vertical	"	73	"	Nose-on Broadside Tail-on	37 1100 25	A53
B-47	SHF Radar	--	Dynamic	9375	Pulse	Nose-on Broadside Tail-on	24 178 12	A54
B-50 (model)	Hybrid T	Horizontal	Static	73	CW	Nose-on Broadside Tail-on	100 1090 225	A55
"	"	Vertical	"	73	"	Nose-on Broadside Tail-on	64 900 40	A55
Cessna	Advanced Development System D2-1	--	Dynamic	10,000	--	--	14 (av)	A42
"	--	--	"	--	--	Approaching and Receding	9.5	A35, A36
Curtiss-Wright 15-D	--	--	"	--	--	Approaching and Receding	23	A35, A36

Table A-3: Aircraft Cross-Sections (Cont.)

Body	Equipment	Polarization	Static or Dynamic	Frequency (in mc/s)	CW or Pulse	Aspect	Radar Cross-Section (in m^2)	Ref
Curtiss-Wright 15-D	Advanced Development System D2-1	--	Dynamic	10,000	--	All	24	A42
"	Advanced Development System J1-1	--	"	3000	--	All	18	A43
F-51	TPS-1B	Horizontal	"	1250	Pulse	Az. $16^\circ - 20^\circ$ Elev. $3^\circ - 6^\circ$	0.13	A50
"	"	"	"	1250	"	Az. $22^\circ - 32^\circ$ Elev. $7^\circ - 11^\circ$	0.5	A50
"	"	"	"	1250	"	All	>1.3	A56
"	"	"	"	1250	"	All (except Az. $85^\circ - 90^\circ$ and $95^\circ - 100^\circ$)	0.9	A56
F-51 (model)	--	"	Static	2600	"	Nose-on Broadside Tail-on	35 380 0.14	A57
"	--	Vertical	"	2600	"	Nose-on Broadside Tail-on	60 560 0.16	A57
F-51	SP-1M	Horizontal	Dynamic	2810	"	Az. $16^\circ - 20^\circ$ Elev. $3^\circ - 6^\circ$	6	A50

Table A-3: Aircraft Cross-Sections (Cont.)

Body	Equipment	Polarization	Static or Dynamic	Frequency (in mc/s)	CW or Pulse	Aspect	Radar Cross-Section (in m^2)	Ref
F-51	SP-1M	Horizontal	Dynamic	2810	Pulse	Az. 22° - 32° Elev. 7° - 11°	0.5	A50
"	"	"	"	2810	"	All	4.8	A56
"	"	"	"	2810	"	All (except Az. 85° - 90° and 95° - 100°)	2.3	A56
"	MK-33	"	"	9380	"	All	8.3	A56
"	"	"	"	9380	"	All (except Az. 85° - 90° and 95° - 100°)	4.6	A56
"	TS-35A*	--	"	--	"	--	1.8	A45
F-80 (with wing tanks)	TPS-1B	Horizontal	"	1250	"	Az. 349° - 359° Elev. 1° - 7°	1	A46
"	SP-1M	"	"	2810	"	Az. 349° - 359° Elev. 1° - 7°	1.6	A46
F-80 (without wing tanks)	TPS-1B	"	"	1250	"	Az. 333° - 356° Elev. 3° - 12°	1.3	A46

*Actually consisted of the TS-35A test set (used both as a power meter and a signal generator), antenna, directional coupler, waveguide, receiver, and "A" scope.

Table A-3: Aircraft Cross-Sections (Cont.)

Body	Equipment	Polarization	Static or Dynamic	Frequency (in mc/s)	CW or Pulse	Aspect	Radar Cross-Section (in m^2)	Ref
F-80 (without wing tanks)	SP-1M	Horizontal	Dynamic	2810	Pulse	Az. 333° - 356° Elev. 3° - 12°	1.5	A46
F-80	APG-33	--	"	--	"	Nose-on	0.19	A41
F-80 (model)	--	Horizontal	Static	2600	"	Nose-on Broadside Tail-on	4 50 1.8	A58
"	--	Vertical	"	2600	"	Nose-on Broadside Tail-on	3.2 100 1.4	A58
F-84 (model)	AN/TPQ-2	Horizontal	"	2600	"	Nose-on Broadside Tail-on	5.6 225 16	A59
"	"	Vertical	"	2600	"	Nose-on Broadside Tail-on	10 100 17	A59
"	Hybrid T	Horizontal	"	73	CW	Nose-on Broadside Tail-on	49 156 36	A60
"	"	Vertical	"	73	"	Nose-on Broadside Tail-on	1.4 144 5.8	A60
"	"	Horizontal	"	73	"	Nose-on Broadside Tail-on	42 240 42	A60

Table A-3: Aircraft Cross-Sections (Cont.)

Body	Equipment	Polarization	Static or Dynamic	Frequency (in mc/s)	CW or Pulse	Aspect	Radar Cross-Section (in m^2)	Ref
F-84 (model)	Hybrid T	Vertical	Static	73	CW	Nose-on Broadside Tail-on	0.64 196 1.6	A60
F-86 (model)	--	Horizontal	"	73	"	Nose-on Broadside Tail-on	0.1 130 0.9	A61
"	Hybrid T	"	"	200	"	Nose-on Broadside Tail-on	1.4 55 3.8	A62, A63
"	"	Vertical	"	200	"	Nose-on Broadside Tail-on	4.4 100 0.3	A62, A63
"	"	Horizontal	"	545	"	Nose-on Broadside Tail-on	12 300 36	A62, A63
"	"	Vertical	"	545	"	Nose-on Broadside	9.8 500	A62, A63
"	"	Horizontal	"	1200	"	Nose-on Broadside Tail-on	1.8 300 4	A62, A63
"	"	Vertical	"	1200	"	Nose-on Broadside	13 300	A62, A63
F-86	TPS-1B	Horizontal	Dynamic	1250	Pulse	All	6.7	A64

Table A-3: Aircraft Cross-Sections (Cont.)

Body	Equipment	Polarization	Static or Dynamic	Frequency (in mc/s)	CW or Pulse	Aspect	Radar Cross-Section (in m^2)	Ref
F-86 (model)	AN/TPQ-2	Horizontal	Static	2600	Pulse	Nose-on Broadside Tail-on	0.2 210 1.4	A65
"	"	Vertical	"	2600	"	Nose-on Broadside Tail-on	0.23 130 1	A65
F-86	SP-1M	Horizontal	Dynamic	2810	"	All	12	A64
"	--	--	"	9375	"	Nose-on Broadside Tail-on	3 31 20	A66
"	MK-33	Horizontal	"	9380	"	All	5.7	A64
F-86 (with wing tanks)	TPS-1B	Horizontal	"	1250	"	Az. 357^{o} - 3^{o} Elev. 2^{o} - 10^{o}	1.6	A50
"	SP-1M	"	"	2810	"	Az. 357^{o} - 3^{o} Elev. 2^{o} - 10^{o}	2.3	A50
V-formation of three F-86's	TPS-1B	Horizontal	"	1250	"	Az. 359^{o} - 6^{o} Elev. 2^{o} - 10^{o}	1	A46
"	"	"	"	1250	"	All	10	A67

Table A-3: Aircraft Cross-Sections (Cont.)

Body	Equipment	Polarization	Static or Dynamic	Frequency (in mc/s)	CW or Pulse	Aspect	Radar Cross-Section (in m^2)	Ref
V-formation of three F-86's	SP-1M	Horizontal	Dynamic	2810	Pulse	Az. 359° - 6° Elev. 2° - 10°	16	A46
"	"	"	"	2810	"	All	50	A67
"	MK-33	"	"	9380	"	All	9.2	A67
Havoc (A-20) (model)	Hybrid T	"	Static	600	CW	Approaching Receding	3.2 0.03	A36, A39
"	"	Vertical	"	600	"	Approaching Receding	1.9 0.02	A36, A39
"	--	Horizontal	"	600	--	Approaching Receding	2.8 0.092	A36, A40
"	--	Vertical	"	600	--	Approaching Receding	0.84 0.009	A36, A40
"	Radar AA no. 3 Mk 2	--	Dynamic	S-band	Pulse	Approaching Receding	33 15	A68
J2F	Advanced Development System J1-1	--	"	3000	--	All	32	A43

Table A-3: Aircraft Cross-Sections (Cont.)

Body	Equipment	Polarization	Static or Dynamic	Frequency (in mc/s)	CW or Pulse	Aspect	Radar Cross-Section (in m^2)	Ref
J2F	Advanced Development System D2-1	--	Dynamic	10,000	--	All	39	A42
"	Radar (type unknown)	--	"	--	--	All	41	A34
"	--	--	"	--	--	Approaching and Receding	25	A35, A36
JRF	--	--	"	--	--	Approaching and Receding	30	A35, A36
Lancaster	--	45°	"	1200	--	Approaching Receding	265 127	A69
"	Radar AA No. 3 Mk 2	--	"	S-band	Pulse	Approaching Receding	147 70	A68
"	--	45°	"	S-band	--	Approaching Receding	234 102	A69
"	Radar AA No. 3 Mk 7	--	--	X-band	--	Nose-on Broadside Tail-on	172 930 64	A70
Lincoln	"	--	Dynamic	X-band	--	Nose-on Tail-on	380 44	A70

Text A-3: Aircraft Cross-Sections (Cont.)

Body	Equipment	Polarization	Static or Dynamic	Frequency (in mc/s)	CW or Pulse	Aspect	Radar Cross-Section (in m^2)	Ref
Meteor	--	45°	Dynamic	1200	--	Approaching Receding	6.1 4.5	A69
"	--	45°	"	S-band	--	Approaching Receding	7.1 4.4	A69
"	Radar AA No. 3 Mk 2	--	"	S-band	Pulse	Approaching Receding	10 3	A71
"	Radar AA No. 3 Mk 7	--	--	X-band	--	Nose-on Tail-on	7 2.5	A70
Mosquito	--	45°	Dynamic	1200	--	Approaching Receding	18 14	A69
"	--	45°	"	S-band	--	Approaching Receding	15 9.6	A69
"	Radar AA No. 3 Mk 2	--	"	S-band	Pulse	Approaching Receding	19 11	A68
"	Radar AA No. 3 Mk 7	--	--	X-band	--	Nose-on Broadside Tail-on	15 88 8	A70

Table A-3: Aircraft Cross-Sections (Cont.)

Body	Equipment	Polarization	Static or Dynamic	Frequency (in mc/s)	CW or Pulse	Aspect	Radar Cross-Section (in m^2)	Ref
MX-1626 (with pod) (model)	Hybrid T	Horizontal	Static	75	CW	Nose-on Broadside Tail-on	115 485 9	A72
"	"	Vertical	"	75	"	Nose-on Broadside Tail-on	12 2100 1	A72
MX-1626 (without pod) (model)	"	Horizontal	"	75	"	Nose-on Broadside Tail-on	100 196 25	A72
"	"	Vertical	"	75	"	Nose-on Broadside Tail-on	4 575 0.25	A72
MX-1626 pod (model)	"	Horizontal	"	75	"	Nose-on Broadside Tail-on	9 250 2.3	A72
"	"	Vertical	"	75	"	Nose-on Broadside Tail-on	0.25 272 0.25	A72
O-47	Advanced Development System D2-1	--	Dynamic	10,000	--	--	12 (av)	A42
"	--	--	"	--	--	Approaching and Receding	10	A35, A36
OS-2U	Advanced Development System J1-1	--	"	3000	--	All	13	A43

Table A-3: Aircraft Cross-Sections (Cont.)

Body	Equipment	Polarization	Static or Dynamic	Frequency (in mc/s)	CW or Pulse	Aspect	Radar Cross-Section (in m^2)	Ref
OS-2U	Advanced Development System D2-1	--	Dynamic	10,000	--	All	12	A42
"	--	--	"	--	--	Approaching and Receding	9.5	A35, A36
OS-2V	Radar (type unknown)	--	"	--	--	All	16	A34
P-38	Radar (type unknown)	--	"	--	--	All	5.4	A34
P-47	Advanced Development System D2-1	--	"	10,000	--	--	16	A42
"	Radar (type unknown)	--	"	--	--	All	8	A34
"	TS-35A*	--	"	--	Pulse	--	13	A45
P-61	"	--	"	--	"	--	26	A45

*Actually consisted of the TS-35A test set (used both as a power meter and a signal generator), antenna, directional coupler, waveguide, receiver, and "A" scope.

Table A-3: Aircraft Cross-Sections (Cont.)

Body	Equipment	Polarization	Static or Dynamic	Frequency (in mc/s)	CW or Pulse	Aspect	Radar Cross-Section (in m^2)	Ref
P-80 (photo equipped)	APG-16	Horizontal	Dynamic	X-band	--	Approaching	0.13 (mean)	A33
P-80 (with wing tanks)	"	"	"	X-band	--	Approaching	0.28 (mean)	A33
P-80	"	Circular	"	X-band	--	Approaching Broadside (approx) Receding	0.06 0.92 (mean) 1 (mean)	A33
"	"	Horizontal	"	X-band	--	Broadside (approx) Receding	10 1.7 (mean)	A33
"	"	Vertical	"	X-band	--	Approaching Broadside (approx) Receding	0.24 10 (mean) 2.3 (mean)	A33
"	"	Horizontal	"	X-band	--	Circle at one to two miles with steep bank	1.5 (mean)	A33
"	TS-35A*	--	"	--	Pulse	--	0.19	A45
PBY	Radar (type unknown)	--	"	--	--	All	52	A34
"	--	--	"	--	--	Approaching and Receding	31	A35, A36

*Actually consisted of the TS-35A test set (used both as a power meter and a signal generator), antenna, directional coupler, waveguide, receiver, and "A" scope.

Table A-3: Aircraft Cross-Sections (Cont.)

Body	Equipment	Polarization	Static or Dynamic	Frequency (in mc/s)	CW or Pulse	Aspect	Radar Cross-Section (in m^2)	Ref
R.T.V.1 or Lop/Gap	Radar AA No. 4 Mk 3	--	Dynamic	212	Pulse	All	1.5 (mean)	A73
SNB	Radar (type unknown)	--	"	--	--	All	21	A34
SNC	Advanced Development System D2-1	--	"	10,000	--	All	6.2	A42
"	--	--	"	--	--	Approaching and Receding	3.9	A35, A36
SNJ	--	--	"	--	--	Approaching and Receding	5	A35, A36
Spitfire	Radar AA No. 3 Mk 2	--	"	S-band	Pulse	Approaching Receding	13 5	A68
SWB	--	--	"	--	--	Approaching and Receding	13	A35, A36
Taylorcraft	Advanced Development System D2-1	--	"	10,000	--	All	19	A42
"	Radar (type unknown)	--	"	--	--	All	16	A34

Table A-3: Aircraft Cross-Sections (Cont.)

Body	Equipment	Polarization	Static or Dynamic	Frequency (in mc/s)	CW or Pulse	Aspect	Radar Cross-Section (in m^2)	Ref
Taylorcraft	--	--	Dynamic	--	--	Approaching and Receding	9.5	A35, A36
Tempest	--	45^o	"	1200	--	Approaching Receding	5.7 4.2	A69
"	--	45^o	"	S-band	--	Approaching Receding	5.8 3.5	A69
Valiant	Radar AA No. 3 Mk 7	--	--	X-band	--	Nose-on Tail-on	98 196	A70
Vampire (model)	Hybrid T	Horizontal	Static	400	CW	Nose-on Broadside Tail-on	5 100 7.5	A62, A63
"	"	Vertical	"	400	"	Nose-on Broadside Tail-on	3.1 80 2	A62, A63
"	"	Horizontal	"	1090	"	Nose-on Broadside Tail-on	1.4 60 11	A62, A63
"	"	Vertical	"	1090	"	Nose-on Broadside Tail-on	16 60 2.5	A62, A63
"	"	Horizontal	"	2400	"	Nose-on Broadside Tail-on	4 60 3	A62, A63

Table A-3: Aircraft Cross-Sections (Cont.)

Body	Equipment	Polarization	Static or Dynamic	Frequency (in mc/s)	CW or Pulse	Aspect	Radar Cross-Section (in m^2)	Ref
Vampire (model)	Hybrid T	Vertical	Static	2400	CW	Nose-on Broadside Tail-on	1.5 50 4	A62, A63
Vampire	--	45^o	Dynamic	1200	--	Approaching Receding	6.6 4.3	A69
"	--	45^o	"	S-band	--	Approaching Receding	8 3.3	A69
"	--	45^o	"	S-band	--	Approaching Receding	6.6 4.1	A69
Wellington	Radar AA No. 3 Mk 2	--	"	S-band	Pulse	Approaching Receding	110 79	A68
"	"	--	"	S-band	"	Approaching Receding	122 75	A68

Table A-4: Cross-Sections of Simple Geometrical Shapes

Body	Equipment	Polarization	Static or Dynamic	Frequency (in mc/s)	CW or Pulse	Aspect	Radar Cross-Section (in m^2)	Ref
Cone (Alt. = 6" dia. of base = $3\frac{11}{32}$")	AN/TPQ-2	Horizontal	Static	23,870	Pulse	Nose-on	3×10^{-8}	A15
Cone (Alt. = 6" dia. of base = $2\frac{1}{32}$")	Pulsed Radar Method	--	"	"	"	Nose-on	$2.54\ \lambda^2$	A15
Cone (Alt. = 6" dia. of base = $1\frac{1}{32}$")	"	"	"	"	"	Nose-on	$0.57\ \lambda^2$	A15
40° Cone*	Standing Wave	--	"	--	--	Nose-on	$1.1 \times 10^{-3}\ \lambda^2$	A74
50° Cone*	"	--	"	--	--	Nose-on	$1.6 \times 10^{-3}\ \lambda^2$	A74
65° Cone*	"	--	"	--	--	Nose-on	$4.8 \times 10^{-2}\ \lambda^2$	A74
65° Cone* (large wooden metalized surface)	--	--	"	--	--	Nose-on	$0.058\ \lambda^2$ (av)	A75
Cone 0.588" 1.625"	Doppler Radar	Vertical	Static Doppler	23,700	--	Nose-on	8.7×10^{-5}	A21
Cylinder (length = 1.5" diameter = 0.588")	"	"	"	"	--	Nose-on	2.5×10^{-3}	A21

*Angle represents 1/2 cone angle.

Table A-4: Cross-Sections of Simple Geometrical Shapes (Cont.)

Body	Equipment	Polarization	Static or Dynamic	Frequency (in mc/s)	CW or Pulse	Aspect	Radar Cross-Section (in m^2)	Ref
Cylinder (length = 6-1/8" radius = 2.8 λ)	AN/TPQ-2	Horizontal	Static	23,870	Pulse	Perpendicular to axis of cylinder	0.5	A15
Cone-Cylinder (max. dia. = 0.588" tot. lgth. = 3.125" cyl. lgth. = 1.5")	Doppler Radar	Vertical	Static Doppler	23,700 S-band (phase) K-band (amp.)	--	Nose-on	9.8×10^{-3} 2.5×10^{-4}	A21
Cone-Cylinder (max. dia. = 4.7" tot. lgth. = 25" cyl. lgth. = 12")	"	"	"	23,700 S-band (phase) K-band (amp.)	--	Nose-on	1×10^{-2} 1.4×10^{-2}	A21
Flat Plate (10 cm. sq.)	Hybrid T	--	Static	3000	CW	Perpendicular to Plate	0.111	A76
Flat Plate (3" by 1-1/4")	AN/TPQ-2	Horizontal	"	23,870	Pulse	Perpendicular to Plate	0.25	A15
Flat Plate (polystyrene 4" sq. 1/8" thick)	Hybrid T	--	"	S-band	CW	Perpendicular to Plate	0.0324	A77
10 cm ogive max. dia. = 2.05 cm	"	Vertical	"	3000	"	Broadside	5.1×10^{-4} (max. echo area)	A77
"	"	Horizontal	"	"	"	Broadside	6.9×10^{-3} (max. echo area)	A77
"	"	"	"	"	"	Nose-on	1.5×10^{-6}	A77

Table A-4: Cross-Sections of Simple Geometrical Shapes (Cont.)

Body	Equipment	Polarization	Static or Dynamic	Frequency (in mc/s)	CW or Pulse	Aspect	Radar Cross-Section (in m^2)	Ref
20 cm ogive (max. dia. = 5.18 cm)	Hybrid T	Vertical	Static	3000	CW	Broadside	1×10^{-2} (max. echo area)	A77
"		Horizontal		3000		Broadside	2.67×10^{-2}	A77
"	"	"	"	3000	"	Nose-on	1.7×10^{-6}	A77
30° ogive*	(Ground Plane)	"	"	--		Nose-on	3.3×10^{-7}	A78
30° ogive*	Standing Wave	--	"	--	--	Nose-on	$1.3 \times 10^{-4} \lambda^2$	A75
40° ogive*	"	--	"	--	--	Nose-on	$5.3 \times 10^{-4} \lambda^2$	A74
Sphere (radius = 1.6 cm)	Hybrid T	--	"	3000	CW	--	3.014×10^{-3}	A39
Sphere (radius = 1.32 cm)	"	--	"	9000		--	3.49×10^{-4}	A76
Sphere (radius = 4 cm)	"	--	"	3000		--	3.14×10^{-3}	A76

*Angle represents 1/2 tangent cone angle.

Table A-4: Cross-Sections of Simple Geometrical Shapes (Cont.)

Body	Equipment	Polarization	Static or Dynamic	Frequency (in mc/s)	CW or Pulse	Aspect	Radar Cross-Section (in m^2)	Ref
Sphere (radius = 3")	Bistatic Radar	Horizontal	Static	3000	CW	σ (0) σ (90°) σ (180°)	2.56×10^{-2} 1.47×10^{-2} 0.47	A79
"	"	Vertical	"	3000	"	σ (0) σ (90°) σ (180°)	2.56×10^{-2} 1.87×10^{-2} 0.47	A79
Sphere (radius = 8.6 cm)	Hybrid T	--	"	3000	"	--	3.5168×10^{-2}	A80
Sphere (radius = 2.5")	"	--	"	9800	"	--	1.29×10^{-2}	A81
Sphere (radius = 3")	Bistatic Radar	Vertical	"	9375	"	σ (90°) σ (-90°)	1.45×10^{-2} 1.25×10^{-2}	A82
Sphere (radius = 9")	--	--	"	K-band	--	--	0.14	A83
Balloon with conducting paint (radius = 18')	--	--	Dynamic	K-band	--	--	0.283	A83
Sphere (radius = 1")	Standing wave half space over ground plane	--	Static	--	--	--	7.28×10^{-3}	A80
Sphere (water and styrofoam, radius = 3.2 cm)		--	"	--	--	--	1.55×10^{-2}	A80

Table A-4: Cross-Sections of Simple Geometrical Shapes (Cont.)

Body	Equipment	Polarization	Static or Dynamic	Frequency (in mc/s)	CW or Pulse	Aspect	Radar Cross-Section (in m^2)	Ref
Sphere (polystyrene radius = 1/2")	Hybrid T	--	Static	3000	CW	--	7.17×10^{-5}	A84
Sphere (polystyrene radius = 1")	"	--	"	3000	"	--	1.43×10^{-4}	A84
Sphere (polystyrene radius = 1-1/4")	"	--	"	3000	"	--	1.52×10^{-4}	A84
Sphere (polystyrene radius = 1-1/2")	"	--	"	3000	"	--	2.06×10^{-3}	A84
Sphere (polystyrene radius = 2")	"	--	"	3000	"	--	1.25×10^{-2}	A84
Wedge* (included angle = 20°)	Parallel Plates (standing wave method)	Parallel to axis of wedge	"	--	"	Perpendicular to edge and in plane of symmetry of wedge	1.04×10^{-3} 1.02×10^{-3} 8.7×10^{-4}	A78
Wedge* (included angle = 30°)	"	"	"	--	"	"	1.17×10^{-3} 1.12×10^{-3} 1.18×10^{-3} 1.28×10^{-3}	A78
Wedge* (included angle = 45°)	"	"	"	--	"	"	1.9×10^{-3} 1.75×10^{-3} 1.61×10^{-3} 1.7×10^{-3}	A78
Wedge* (included angle = 60°)	"	"	"	--	"	"	1.18×10^{-3} 1.25×10^{-3} 1.42×10^{-3} 1.26×10^{-3}	A78

*Radar cross-section given as cross-section per unit length of wedge (square meters per meter).

Table A-4: Cross-Sections of Simple Geometrical Shapes (Cont.)

Body	Equipment	Polarization	Static or Dynamic	Frequency (in mc/s)	CW or Pulse	Aspect	Radar Cross-Section (in m^2)	Ref
Wedge* (included angle = 70^o)	Parallel Plates (standing wave method)	Parallel to axis of wedge	Static	--	CW	Perpendicular to edge and in plane of symmetry of wedge	1.56×10^{-3} 1.47×10^{-3} 1.54×10^{-3}	A78
Wedge* (included angle = 80^o)	"	"	"	--	"	"	1.71×10^{-3} 1.74×10^{-3} 2.8×10^{-3}	A78

*Radar cross-section given as cross-section per unit length of wedge (square meters per meter).

REFERENCES

FOR APPENDIX A

A1 Siegel, K. M., Crispin, J. W., and Kleinman, R. E., "Studies In Radar Cross-Section VII, Summary of Radar Cross-Section Studies Under Project Wizard," Willow Run Research Center, University of Michigan, Report UMM-108, November 1952. SECRET.

A2 Meeks, M. L., Logan, N. A., Brewer, H. R., and Wilcox, C. H., "A Bibliography of Radar Reflection Characteristics Vol. I," State Engineering Experiment Station, Georgia Institute of Technology, 1952. RESTRICTED.

A3 Meeks, M. L., Logan, N. A., Brewer, H. R., and Wilcox, C. H., "A Bibliography of Radar Reflection Characteristics Vol. II," State Engineering Experiment Station, Georgia Institute of Technology, 1952. CONFIDENTIAL.

A4 Meeks, M. L., Logan, N. A., Brewer, H. R., and Wilcox, C. H., "A Bibliography of Radar Reflection Characteristics Vol. III," State Engineering Experiment Station, Georgia Institute of Technology, 1952. SECRET.

A5 "Back Scattering Coefficient Patterns of Rocket Shells for 20 MC," Ohio State University Research Foundation, Report-302-15, (ATI-49022), August 1948. CONFIDENTIAL.

A6 "Back Scattering Coefficient Patterns of Rocket Shells for 50 MC," Ohio State University Research Foundation, Report-302-16, (ATI-48939), August 1948. CONFIDENTIAL.

A7 "Back Scattering Coefficient Patterns of Rocket Shells for 100 MC," Ohio State University Research Foundation, Report-302-17, September 1948. CONFIDENTIAL.

A8 "Back Scattering Coefficient Patterns of Rocket Shells for 300 MC," Ohio State University Research Foundation, Report-302-18, (ATI-40573), September 1948. CONFIDENTIAL.

A9 "Echo Patterns of Rocket Shells for 600 MC," Ohio State University Research Foundation, Report-302-20, (ATI-42137), October 1948. CONFIDENTIAL.

A10 "Echo Patterns of Rocket Shells for 1200 MC," Ohio State University Research Foundation, Report-308-23, (ATI-49037), November 1948. CONFIDENTIAL.

A11 Linderman, O. E., "Project Thumper: Missile Echoing Area," General Electric Company, Report GE-TR-55408, June 1948. SECRET.

A12 "Radar System Analysis Comparative-Performance Study of Pulse, F-M and Doppler Techniques for Ground-Based Long-Range Search and M.T.I. Radar Systems," Sperry Gyroscope Co., Report Sperry-5223-1109, (ATI-52865), June 1948. SECRET.

A13 "Determination of Echoing Area Characteristics of Various Objects Fourteenth Quarterly Progress Report," Ohio State University Research Foundation, Report-302-36, August 1950. CONFIDENTIAL.

A14 "Determination of Back Scattering Coefficients of Various Objects," Ohio State University Research Foundation, Report-302-10, (ATI-28341), May 1948. CONFIDENTIAL.

A15 Sichak, W., "Missile Detection Final Report," Federal Telecommunications Laboratory, Report ATI-42811, August 1948. SECRET.

A16 MacDonald, F. C., "Radar Area Measurements of V-2 Rockets," Naval Research Laboratory, NRL Report-3220, January 1948. RESTRICTED.

A17 MacDonald, F. C., "Measurements of Radar Area of a V-2 Rocket," Naval Research Laboratory, Report NRL-C-3460-52/48A. (ATI-105502), August 1948. CONFIDENTIAL.

A18 General Electric Company, "The Thumper Project Final Report Phase I," Report ATI-57044, June 1949. SECRET.

A19 "Echoing Areas of Objects Progress Report, 1 November 1948 to 31 December 1948," Ohio State University Research Foundation, Report-302-25, (ATI-68314), January 1949. CONFIDENTIAL.

A20 "Echo Patterns of Tanks and Missiles," Ohio State University Research Foundation, Report-302-26, (ATI-71401), January 1949. CONFIDENTIAL.

A21 "Research Investigation on Counter-Battery and Fire Control Radar," Belmont Radio Corporation, Final Report, May 1948. SECRET.

A22 "Back Scattering Coefficient Patterns of Rifle Shells for 1200 MC," Ohio State University Research Foundation, Report-302-11, (ATI-49021), January 1948. CONFIDENTIAL.

A23 "Back Scattering Coefficient Patterns of Mortar Shells for 200 MC," Ohio State University Research Foundation, Report-302-8, (ATI-28359), November 1947. CONFIDENTIAL.

A24 "Echo Patterns of Mortar Shells for 600 MC," Ohio State University Research Foundation, Report-302-6, (ATI-28358), September 1947. CONFIDENTIAL.

A25 "Echo Patterns of Mortar Shells for 1200 MC," Ohio State University Research Foundation, Report-302-2, June 1947. CONFIDENTIAL.

A26 "Echo Patterns of Mortar Shells for 2900 MC," Ohio State University Research Foundation, Report-302-1, May 1947. CONFIDENTIAL.

A27 "Echo Patterns of Mortar Shells for 9000 MC," Ohio State University Research Foundation, Report-302-4, July 1947. CONFIDENTIAL.

A28 "Back Scattering Coefficients of Mortar Shells for 16,000 MC," Ohio State University Research Foundation, Report-302-30, (ATI-64626). CONFIDENTIAL.

A29 "Echo Patterns of Mortar Shells for 24,000 MC," Ohio State University Research Foundation, Report-302-21, (ATI-43506), October 1948. CONFIDENTIAL.

A30 "Determination of Back-Scattering Coefficients of Various Objects," Ohio State University Research Foundation, Report-302-9, (ATI-23410), January 1948. CONFIDENTIAL.

A31 MacDonald, F. C., "L, S, and X Band Radar Echoes from Rifle Shells," Naval Research Laboratory, Report NRL-3720, August 1950. UNCLASSIFIED.

A32 "Quarterly Progress Report, Project Lincoln," Massachusetts Institute of Technology, Report MIT-LINCOLN-RLE-QPR-1, (ATI-123811), October 1951. SECRET.

A33 Muchmore, R. B., and Weiss, L. H., "Radar Echo Scintillation From P-80 and A-20 Airplanes," Hughes Aircraft Company, Report Hughes-TM-212, November 1948. SECRET.

A34 "Pilotless Aircraft Guidance and Control System Design Handbook," Raytheon Manufacturing Company, Report Ray-172, November 1947. SECRET.

A35 "Summary Technical Report of the Committee on Propagation," National Defense Research Committee, Summary Technical Report CP, Vol. 1, Ch. 10.2, 1946. UNCLASSIFIED.

A36 "Equivalent Echoing Areas of Aircraft, and Characteristics of Aircraft Echoes: A Critical Survey of the Literature," Telecommunications Research Establishment, Report TRE-TN-47, (ATI-83160), October 1949. SECRET.

A37 Jacques, R. B., "B-17E Bomber at 100 MC Reflection Patterns," Ohio State University Research Foundation, Report-759-22, (ATI-14551), March 1944. UNCLASSIFIED.

A38 "Analysis and Application of Measurements of Radar Cross-Section of Airplane Models," Harvard University Radio Research Laboratory, Report 411-157, February 1945. UNCLASSIFIED.

A39 Yates, K. P., "A Continuous-Wave Method of Measuring Radar Cross-Sections and Reflection Patterns by Means of Models," Ohio State University Research Foundation, Report-759-33, (ATI-14550), October 1945. UNCLASSIFIED.

A40 "Analysis and Application of Measurements of Radar Cross-Sections of Airplane Models - II," Harvard University, Radio Research Laboratory, Report-411-157A, September 1945. UNCLASSIFIED.

A41 "Report on Trip to Hughes Aircraft and Rand Corporation," Willow Run Research Center, University of Michigan, Internal Memorandum 59-D-10, December 1951. SECRET.

A42 "Recent Performance of the 3 cm Advanced Development System," Massachusetts Institute of Technology, Report MIT-RL-72-7, June 1943. UNCLASSIFIED.

A43 Linford, L. B., Williams, D., Josephson, V., and Woodcock, W., "A Definition of Maximum Range on Aircraft and Its Quantitative Determination," Massachusetts Institute of Technology, Report MIT-RL-353, (ATI-6010), December 1942. UNCLASSIFIED.

A44 Jacques, R. B., "B-24 Bomber at 100 MC Reflection Patterns," Ohio State University Research Foundation, Report-579-21, (ATI-15557), March 1944. UNCLASSIFIED.

A45 Winn, O. H., "Effective Radar Target Area of Various Types of Aircraft," General Electric Company, EMT-1010, December 1946. CONFIDENTIAL.

A46 Ringwalt, D. L., MacDonald, F. C. and Katzin, M., "Quantitative Measurements of Radar Echoes from Aircraft II," Naval Research Laboratory, Report NRL-C3460-18A/51, March 1951. CONFIDENTIAL.

A47 Ament, W. S., MacDonald, F. C., and Passerini, H. J., "Quantitative Measurements of Radar Echoes from Aircraft XI. B-29," Naval Research Laboratories, NRL Memorandum Report No. 164, May 1953. CONFIDENTIAL.

A48 "Echo Measurements of the B-36 Aircraft," Ohio State University Research Foundation, Data Set 5, June 1952. CONFIDENTIAL.

A49 MacDonald, F. C., "Quantitative Measurements of Radar Echoes from Aircraft," Naval Research Laboratory, Report NRL-C-3460-94A/51, June 1951. CONFIDENTIAL.

A50 Ringwalt, D. L., MacDonald, F. C., and Katzin, M., "Quantitative Measurements of Radar Echoes from Aircraft," Naval Research Laboratory, Report NRL-C-3460-73A/50, (ATI-93449), October 1950. CONFIDENTIAL.

A51 Ament, W. S., Katzin, M., MacDonald, F. C., Passerini, H. J., and Watkins, P. L., "Quantitative Measurements of Radar Echoes from Aircraft V. Correction of X-band Values," Naval Research Laboratories, Report NRL-C-3460-132A/52, October 1952. CONFIDENTIAL.

A52 Ament, W. S., MacDonald, F. C., and Passerini, H. J., "Quantitative Measurements of Radar Echoes from Aircraft VIII. B-45," Naval Research Laboratories, NRL Memorandum Report No. 116, January 1953. CONFIDENTIAL.

A53 "Echo Measurements of the B-47 Aircraft," Ohio State University Research Foundation, Data Set 3, June 1952. CONFIDENTIAL.

A54 Schivley, George W., "Measurements of B-47 Aircraft Dynamic Reflection Characteristics," Wright Air Development Center, Report WADC-TN-WCER-52-1, (ATI-163743), June 1952. CONFIDENTIAL.

A55 "Echo Measurements of the B-50 Aircraft," Ohio State University Research Foundation, Data Set 1, June 1952. CONFIDENTIAL.

A56 Ament, W. S., MacDonald, F. C., and Passerini, H. J., "Quantitative Measurements of Radar Echoes from Aircraft IX. F-51," Naval Research Laboratories, NRL Memorandum Report No. 127, March 1953. CONFIDENTIAL.

A57 "Echo Measurements of the F-51 Aircraft at 2600 MC," Ohio State University Research Foundation, Data Set 9, July 1952. CONFIDENTIAL.

A58 "Echo Measurements of the F-80 Aircraft at 2600 MC," Ohio State University Research Foundation, Data Set 10, August 1952. CONFIDENTIAL.

A59 "Echo Measurements of the F-84 Aircraft at 2600 MC," Ohio State University Research Foundation, Data Set 8, June 1952. CONFIDENTIAL.

A60 "Echo Measurements of the F-84 Aircraft," Ohio State University Research Foundation, Data Set 2, May 1952. CONFIDENTIAL.

A61 "Echo Measurements of the F-86 Aircraft," Ohio State University Research Foundation, Data Set 4, May 1952. CONFIDENTIAL.

A62 Hay, D. R., "Radar Cross-Sections of Aircraft," Eaton Electronics Research Laboratory, McGill University, Report No. 3 on Contract DRB-X-27, June 1952. SECRET.

A63 Woonton, G. A., Hay, D. R., and Hogg, D. C., "Radar Cross-Sections of Aircraft," Eaton Electronics Research Laboratory, McGill University, Report No. 1 on Contract DRB-X-27, October 1951. SECRET.

A64 Ament, W. S., MacDonald, F. C., and Passerini, H. J., "Quantitative Measurements of Radar Echoes from Aircraft VI. Corrected F-86 Amplitude Distribution and Aspect Dependence," Naval Research Laboratories, Report NRL-C-3460-143A/52, December 1952. CONFIDENTIAL.

A65 "Echo Measurements of the F-86 Aircraft at 2600 MC," Ohio State University Research Foundation, Data Set 7, May 1952. CONFIDENTIAL.

A66 Schivley, George W., "Measurements of F-86 Aircraft Dynamic Radar Reflection Characteristics," Aircraft Radiation Laboratory, Wright Air Development Center, Report TN-WCLR-52-2, September 1952. CONFIDENTIAL.

A67 Ament, W. S., MacDonald, F. C., and Passerini, H. J., "Quantitative Measurements of Radar Echoes from Aircraft X. Three F-86 Aircraft in Formation," Naval Research Laboratories, NRL Memorandum Report No. 144, April 1953. CONFIDENTIAL.

A68 Beeching, G. H., and Corcovan, N., "The Characteristics of S-Band Aircraft Echoes with Particular Reference to Radar A.A. No. 3 Mk. 2," Ministry of Supply, ADRDE-Research Report No. 253, (ATI-109830), August 1944. CONFIDENTIAL.

A69 Tomlin, D. H., and Merrifield, C. V. F., "An Interin Report on Aircraft Echo Characteristics at L-Band," Radar Research and Development Establishment, Report RRDE-TN-34, (ATI-84621), April 1949. CONFIDENTIAL.

A70 Hutchinson, G. L., and Caswell, A. F., "Further Measurements of Radar Echoing Areas on X-Band," Royal Aircraft Establishment, Technical Note No. G.W. 175, (ATI-145917), February 1952. SECRET.

A71 Beeching, G. H., "The Characteristics of the S-Band Radar Echoes II - The Jet-Propelled Meteor Aircraft," Radar Research and Development Establishment, Report RRDE-CR-326, (ATI-61518), January 1947. CONFIDENTIAL.

A72 "Echo Measurements of the MX-1626 Aircraft," Ohio State University Research Foundation, Data Set 6, December 1952. CONFIDENTIAL.

A73 Bonelle, G. J., "A Velocity Measuring System for R.T.V. 1 and Similar Projectiles," Radar Research and Development Establishment, RRDE Report No. 358, (ATI-92241), September 1950. SECRET.

A74 Sletten, C. J., "Electromagnetic Scattering from Wedges and Cones," Cambridge Research Center, Report CRC-E5090, July 1952. UNCLASSIFIED.

A75 "Technical Progress Report No. 17 to the Steering Committee from the Antenna Laboratory," Cambridge Research Laboratories, CRL Report No. E3110, April 1951. CONFIDENTIAL.

A76 "Quarterly Progress Report for Period April 1 to July 31, 1947," Ohio State University Research Foundation, Report-302-5, July 1947. CONFIDENTIAL.

A77 "Determination of Echoing Area Characteristics of Various Objects," Ohio State University Research Foundation, Report-302-7, October 1947. CONFIDENTIAL.

A78 "Technical Progress Report No. 16 to the Steering Committee from the Antenna Laboratory," Cambridge Research Laboratories, CRL Report No. E3102, January 1951. CONFIDENTIAL.

A79 "Echoing Area Characteristics of Various Objects: Ninth Quarterly Progress Report," Ohio State University Research Foundation, Report-302-29, May 1949. CONFIDENTIAL.

A80 Aden, A. L., "Electromagnetic Scattering From Metal and Water Spheres," Harvard University, Cruft Laboratories, Technical Report No. 106, (ATI-92016), August 1950. UNCLASSIFIED.

A81 Ringwalt, D. L., "A Model Technique for the Measurement of the Radar Characteristics of Targets," Naval Research Laboratory, NRL Report 3800, (ATI-110653), June 1951. UNCLASSIFIED.

A82 Hamren, S. D., "Scattering from Spheres," University of California, Antenna Laboratory, Report Univ-Calif-AL-171, (ATI-83900), June 1950. UNCLASSIFIED.

A83 "Project NIKE--Technical Report - 15 July 1947," Bell Telephone Laboratories, Inc., July 1947. CONFIDENTIAL.

A84 "Determination of Back Scattering Coefficients of Various Objects," Ohio State University Research Foundation, Report-302-14, (ATI-123923), August 1948. CONFIDENTIAL.

APPENDIX B

THE THEORETICAL APPROXIMATION OF THE RADAR CROSS-SECTION OF VARIOUS MISSILES AND MANNED AIRCRAFT

B.1: Introduction

In the work at the Willow Run Research Center it has been necessary on various occasions to estimate the radar cross-section of various aircraft and missiles. In this appendix the results obtained are summarized and, wherever possible, these theoretical results are compared with experiment. Much work has been done in connection with V-2 type and intercontinental ballistic missiles; it is planned to report this work in a future paper in this Radar Cross-Section series. The methods employed in finding theoretical values of cross-section are briefly discussed in Section B-2. Manned aircraft are considered in Section B-3, and Section B-4 contains the results obtained in the consideration of the cross-section of missiles (excluding ballistic types).

B.2: The Methods Employed in Approximating the Cross-Section of a Missile or an Airplane

The purpose of the following paragraphs is simply to place the theoretical values of radar cross-section which are tabulated below in their proper perspective with respect to experimental values of σ, and to re-emphasize the need for the use of the concept of radar cross-section with appropriate regard for its relation to the properties of the radar system.

In determining the cross-section of a composite body such as those under discussion here it has been assumed that components vibrate in such a manner that their fields can be added in random phase. This assumption leads to a simple addition of the radar cross-sections of the various parts of the body in finding the cross-section of the composite body itself. The following argument shows why "random phase" implies this process of simple addition.

The radar cross-section of an arbitrary surface is given by

$$\sigma = \lim_{r \to \infty} 4\pi r^2 \left| \overline{H}^s / \overline{H}^i \right|^2$$

where r is the distance from the radar to the target and $\overline{H}^s$ and $\overline{H}^i$ are the scattered and incident magnetic field vectors respectively. For convenience we may write

$$\sigma = \left| Ae^{i\phi} \right|^2 = A^2 .$$

Consider the radar cross-sections for two scatterers given by

$$\sigma_1 = \left| A_1 e^{i\phi_1} \right|^2 = A_1^2$$

and

$$\sigma_2 = \left| A_2 e^{i\phi_2} \right|^2 = A_2^2 .$$

The radar cross-section of two scatterers, considered together, is given by

$$\sigma = \left| A_1 e^{i\phi_1} + A_2 e^{i\phi_2} \right|^2 .$$

If the position of one of these scatterers is random relative to the other, the expected value of σ , E (σ), is given by

$$E(\sigma) = \frac{1}{4\pi^2} \int_0^{2\pi} d\phi_2 \int_0^{2\pi} \left(A_1 e^{i\phi_1} + A_2 e^{i\phi_2} \right) \left(A_1 e^{i\phi_2} + A_2 e^{-i\phi_2} \right) d\phi_1$$

$$= A_1^2 + A_2^2 .$$

The procedure used in finding these cross-sections involves considering a target as a combination of simple surfaces such as cylinders, flat plates, prolate spheroids, etc, and then adding the calculated return from each surface.

The justification for a random phase addition of the radar cross-sections of the component scatterers is based upon the fact that the relative positions of the component scatterers (or at least the relative positions of the simple geometric configurations used to approximate them) cannot be precisely determined.

In a more exact treatment, the relative positions of the component scatterers would be specified and an approach such as this would not be appropriate. But this approximate method has achieved a moderate degree of success (Ref. B-1) at large wavelengths (for example, greater than about 1 meter for manned aircraft); hence it is only natural to try to extend this technique into the microwave region. It is important to note that for the longer wavelengths the radar cross-section is dependent upon both wavelength and polarization.

Resonance effects are probably always present in the consideration of conventional aircraft. Experimental values of σ indicate that this quantity is less dependent on polarization and resonance phenomena as the wavelength decreases. Since the approximations of geometrical and physical optics are such that the back scattering σ calculated by these methods does not depend upon either polarization or resonance effects, but does depend upon the relative magnitude of λ and ξ (where ξ is a characteristic dimension of the scattering surface), it is only reasonable to expect a moderate degree of success when extending the above technique into the microwave region (i.e., $\lambda << \xi$).

The advantage of this technique is the relative simplicity of the calculations employing physical and geometrical optics.

It should be noted that, although the calculated values of radar cross-section presented herein in some cases seem high, they are really not incompatible with values encountered in the field. The problem of correlating the analytical and experimental values of radar cross-section fundamentally depends upon three factors: the condition of the equipment; the experimental method employed to observe the radar echo; and the validity of the theoretical results.

During World War II a scientific team from the Radiation Laboratories made measurements of the performance of a number of radar sets and compared their range performance with the laboratory or "ideally maintained and adjusted" value. These results are shown in Figure B.1 and discussed below. From this chart we see that in practice a large percentage of radar systems tested were not working at their calibrated efficiency, but at 10 db or more below. Consequently, the values of σ surmised from operational experience with these systems are too small.

One of the attempts to assign causes for this performance degradation may be found in Reference B-2, wherein the sources are taken to be associated with

1. receiver noise figure,
2. S/N ratio.
3. collapsing loss,
4. beam shape loss,
5. plumbing losses,
6. operator losses, and
7. observer factor.

Though definitions of the above may vary, depending on the facility to assign values for each error in a particular radar, the composite effect is observable and measurable. Losses of 20 to 30 db are not unheard of, and thus with a particular measuring instrument such as a usual field-type radar one may be measuring the properties of instrument plus target, instead of the target alone.

Linford (Ref. B-3) defines the effective radar cross-section as that value of σ obtained from the radar range equation which is exceeded during one-half of a series of measuring time intervals. In this way, as Kerr (Ref. B-1) points out, the essential feature of the probability of detecting the echo is introduced into the value of σ. If desired, the required degree of probability could be modified, and the resulting value of σ would be changed accordingly.

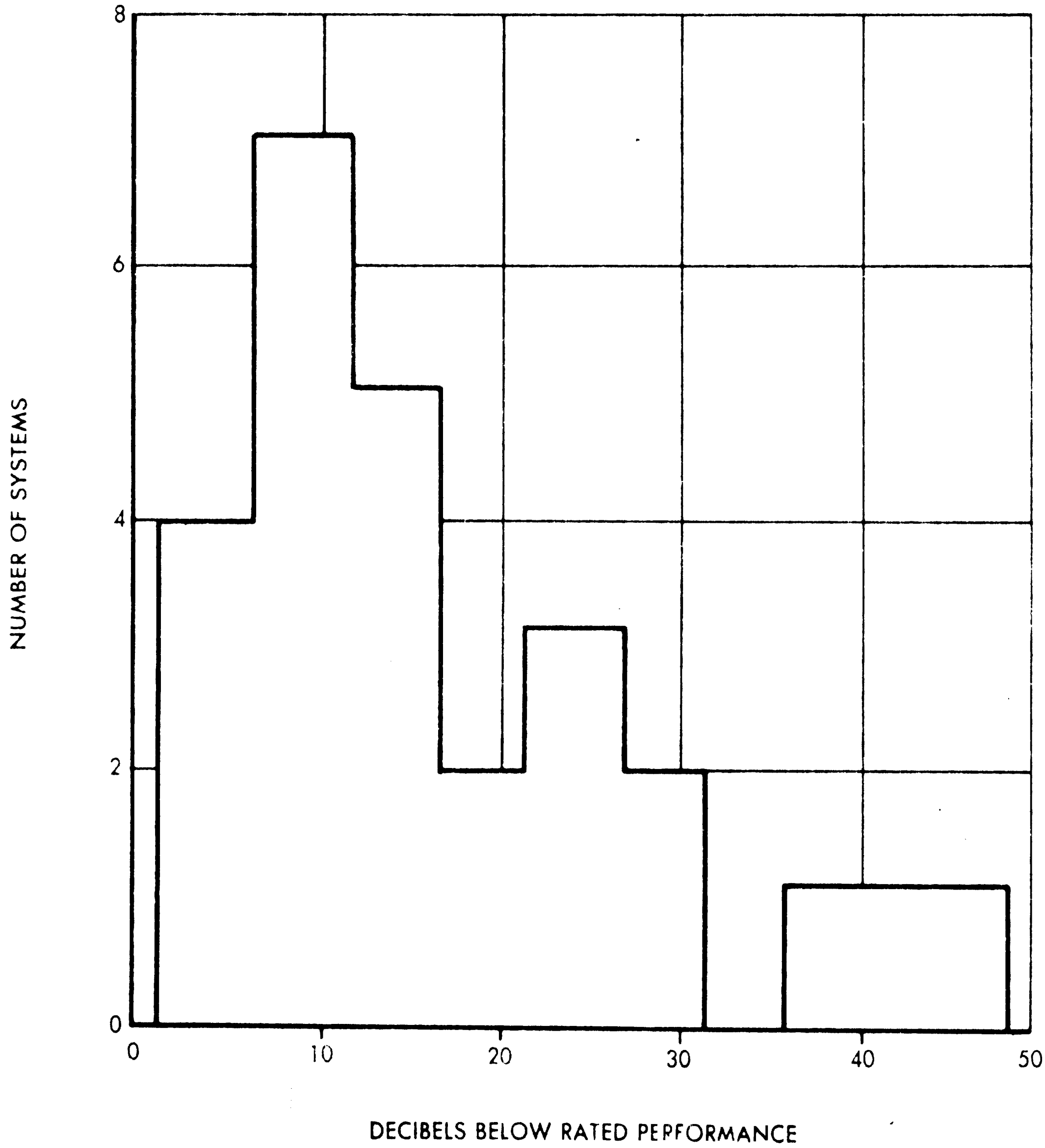

FIG. B-1 RADAR PERFORMANCE SURVEY, JULY 1945
Taken from Radiation Laboratory Series No. 1, "RADAR SYSTEM ENGINEERING". Ridenour, McGraw-Hill, reproduced in Ref. B-2

Another factor important in correlating analytical and experimental values of radar cross-section is the angular variation in target aspect that occurs during the time of observation. This variation may be due to surface vibrations of the scatterer, relative motion between target and radar, etc.

As Barlow and Emerson (Ref. B-2) point out, the probability of detection is dependent upon the nature of the fluctuations of the target signals from scan to scan. They say,

> "A large bomber viewed at the short wavelengths used for A.I. has an echoing area which is such a rapidly varying function of aspect that the inevitable small aspect changes from scan to scan are sufficient to cause considerable fluctuation."

B.3: The Cross-Section of Manned Aircraft

The results obtained for the radar cross-section of the TU-4 (B-29), the IL-28, and the B-47 are tabulated in this section.

Throughout this section the aspect will be specified in terms of ϕ and θ where ϕ is the azimuth angle measured from the nose in the plane of the wing, and θ is the elevation angle measured from the nose in a plane perpendicular to the wing and containing the axis of the fuselage, as illustrated in Figure B-2.

B.3.1: The TU-4 (B-29)

For the purposes of this work, the radar characteristics of the TU-4 are assumed to be essentially the same as those of a B-29, (Ref. B-4).

Applying the techniques briefly outlined in Section B.2 above, the following results were obtained for the aspects defined by $\theta = 0^\circ$ and 4° and $\phi = 0^\circ$ to $\phi = 180^\circ$ at 30° intervals at X-band, S-band, and L-band. The results so obtained are listed below in Table B-1.

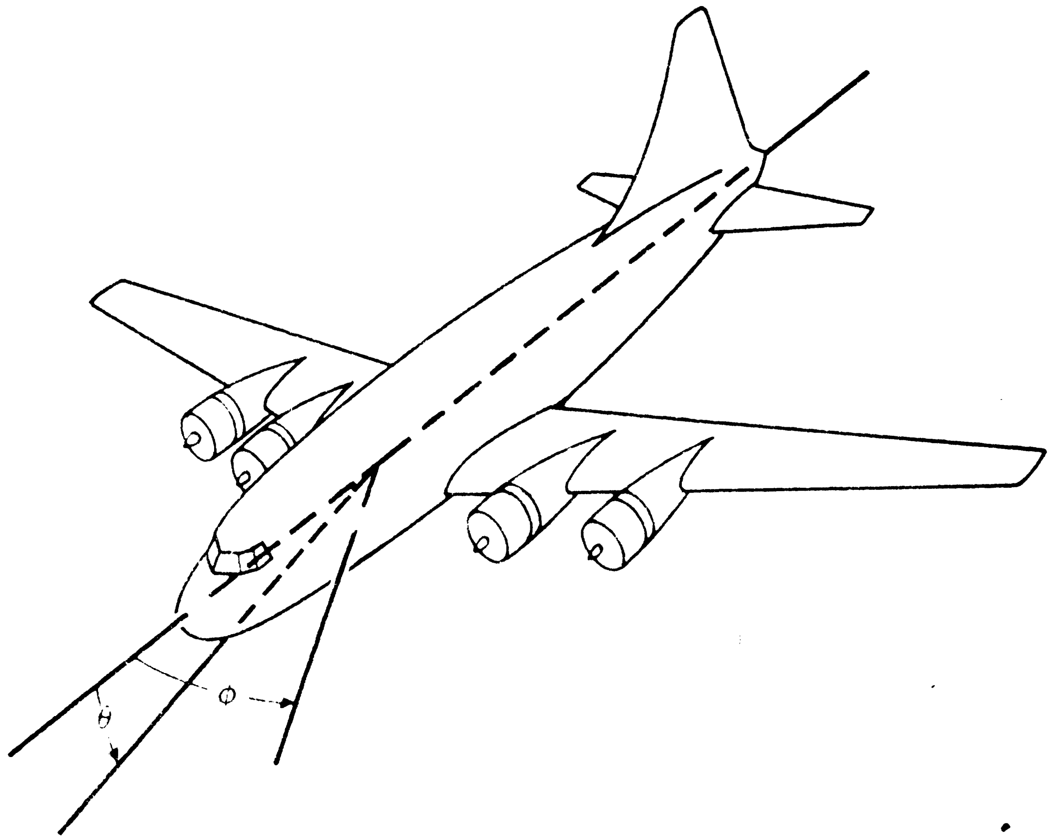

FIG. B-2 BASIC GEOMETRY USED IN DETERMINING THEORETICAL CROSS-SECTIONS OF AIRCRAFT

At the time of the computation of the following data, experimental information could be obtained only for essentially nose-on and tail-on views. Concurrent with the computation of those values a report on the measurement of radar echoes from a B-29 was published at the Naval Research Laboratories (Ref. B-5). A comparison of the theoretical values given below and the NRL experimental values, for comparable aspects, is presented in the following graphs. The graphical method of presentation is the same as that appearing in the NRL report, with the theoretical values added. However, in the following graphs the plotted NRL points are connected to form broken line graphs. Approximately nose-on aspects are shown in Figure B-3, aspects near 30° in azimuth are given in Figure B-4, those near 60° in azimuth are shown in Figure B-5, and Figure B-6 shows the comparison for approximately broadside aspects. Even though small differences exist between the theoretical and experimental aspects compared, examination of the following graphs shows that the predicted values are in general agreement with those obtained experimentally.

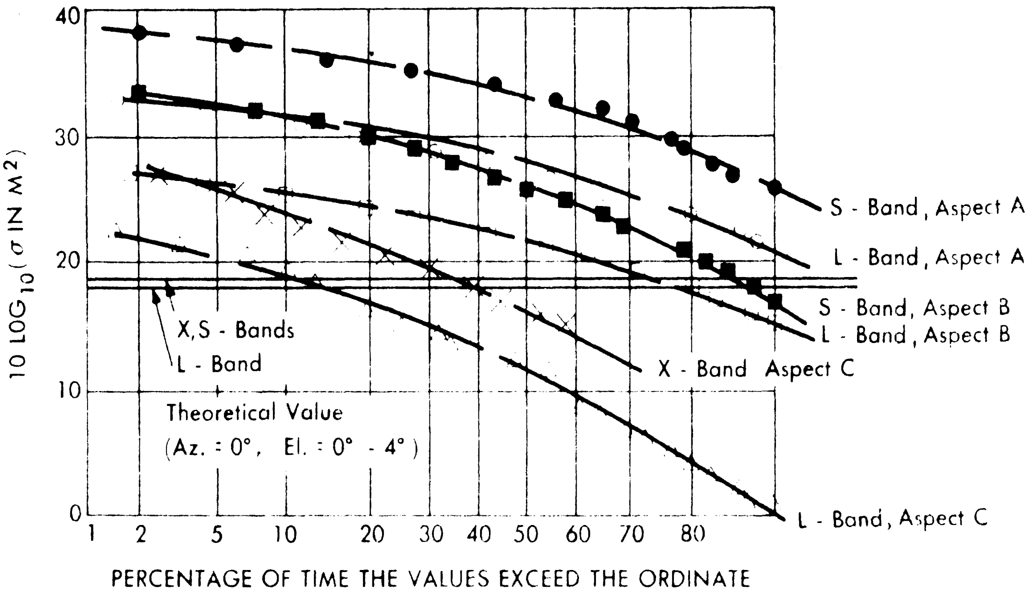

Aspect A: Azimuth 6.59° - 6.75°; Elevation 1.92° - 2.00°
Aspect B: Azimuth 356.08° - 355.83°; Elevation 7.00° - 7.30°
Aspect C: Azimuth 6.17° - 6.25°; Elevation 1.50° - 1.59°

FIG. B-3 COMPARISON OF THEORETICAL AND EXPERIMENTAL CROSS-SECTIONS OF THE B-29 AT ESSENTIALLY NOSE-ON ASPECTS

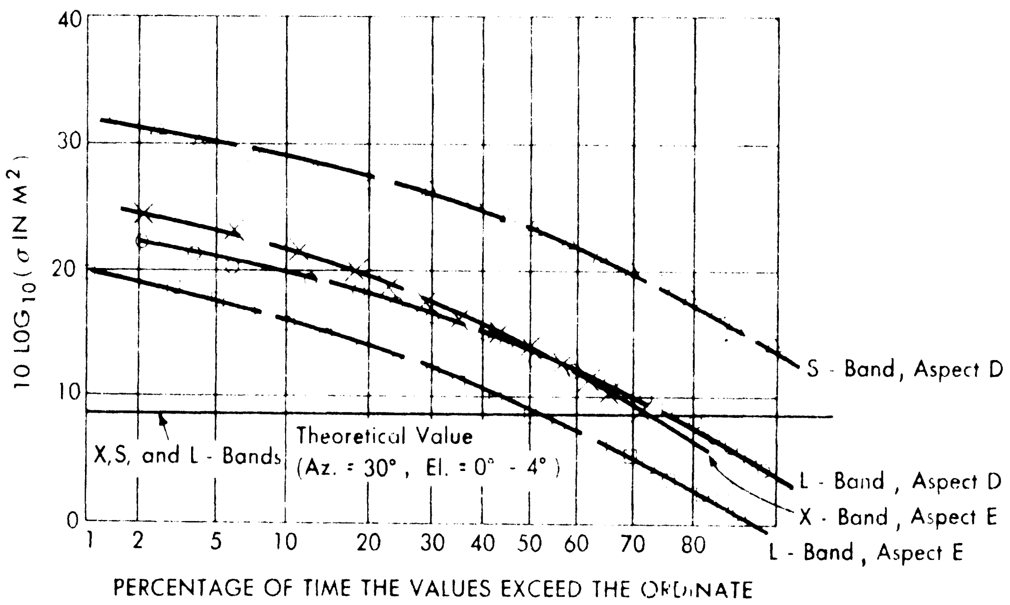

Aspect D: Azimuth 35.0° - 36.75°; Elevation 5.75° - 6.08°
Aspect E: Azimuth 27.0° - 28.08°; Elevation 2.25 - 2.33°

FIG. B-4 COMPARISON OF THEORETICAL AND EXPERIMENTAL CROSS-SECTIONS OF THE B-29 AT THE ASPECT DEFINED BY AZIMUTH ≈30° AND ELEVATION ≈0° - 4°

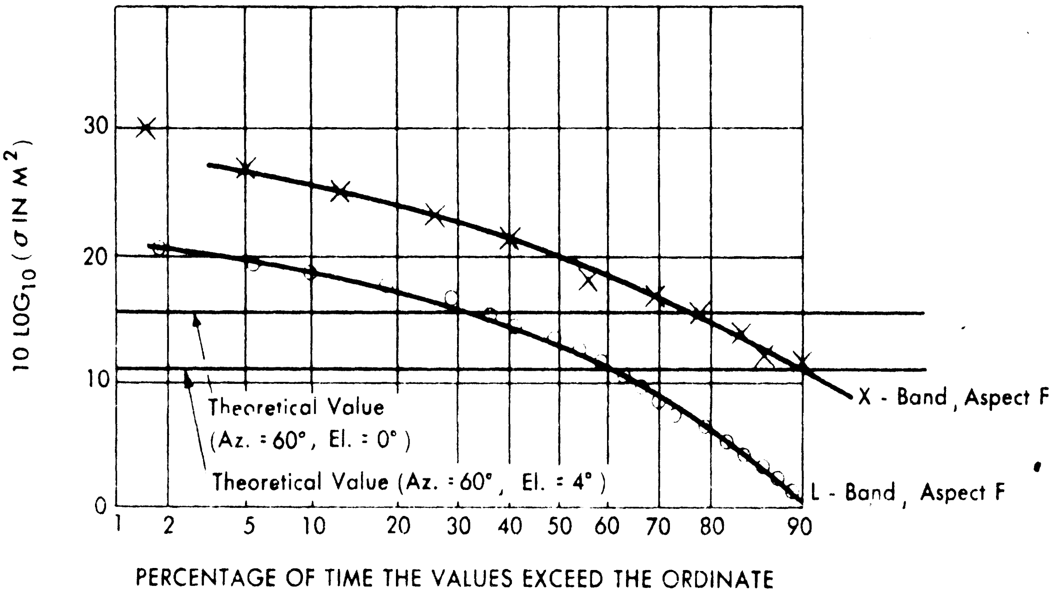

Aspect F: Azimuth 67.50° - 72.00°; Elevation 3.17° - 3.17°

FIG. B-5 COMPARISON OF THEORETICAL AND EXPERIMENTAL CROSS-SECTIONS OF THE B-29 AT THE ASPECT DEFINED BY AZIMUTH≈60° AND ELEVATION≈0° -4°

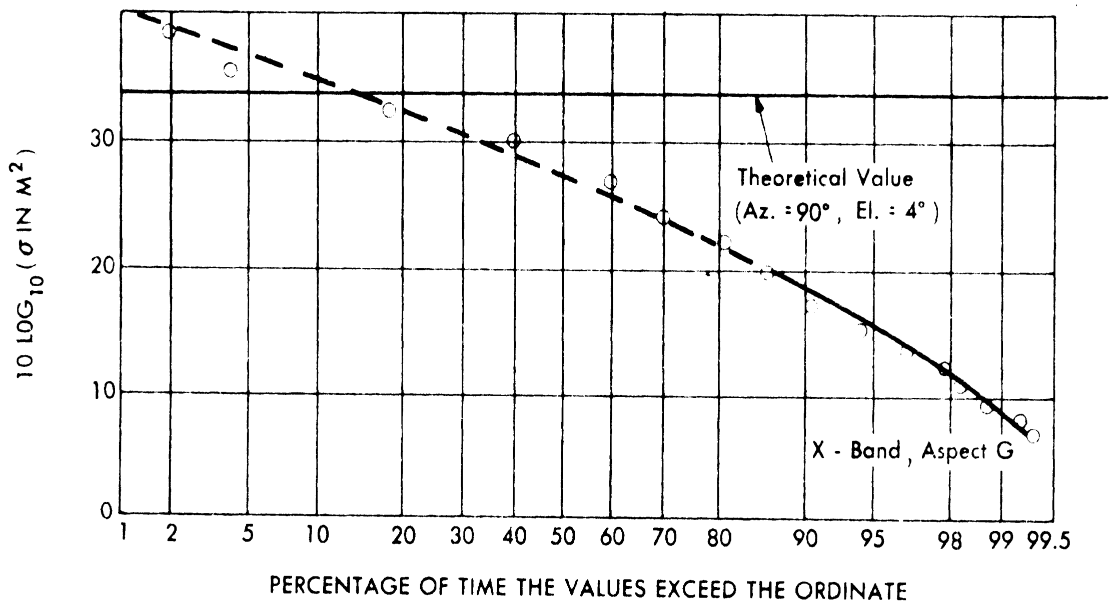

Aspect G: Azimuth 90.00° - 93.08°; Elevation 3.67° - 3.75°

FIG. B-6 COMPARISON OF THEORETICAL AND EXPERIMENTAL CROSS-SECTIONS OF THE B-29 AT THE ASPECT DEFINED BY AZIMUTH≈90° AND ELEVATION≈0° -4°

ASPECT (in degrees)		RADAR CROSS-SECTION IN m^2		
θ	ϕ	X-Band	S-Band	L-Band
0	0	65.1	66.2	68.0
4	0	68.	69.1	70.9
0	30	9.8	9.8	9.8
4	30	6.9	6.9	6.9
0	60	38.4	38.4	38.4
4	60	12.8	12.8	12.8
0	90	2630.	1200.	1370.
4	90	2530.	843.	474.
0	120	32.3	32.3	32.3
4	120	6.7	6.7	6.7
0	150	8.7	8.7	8.7
4	150	5.8	5.8	5.8
0	180	62.6	62.6	62.6
4	180	62.6	62.6	62.6

σ for the TU-4 (B-29)

Table B-1

The monostatic and bistatic radar cross-sections at 600 mc for the TU-4 (B-29) were also computed and compared for one particular aspect. The monostatic radar cross-section, σ_m, and the bistatic radar cross-section, σ_b, were calculated by means of physical and geometrical optics. The target aspect is determined from the geometry in Figure B-7 where points P and Q are 30 miles apart and where the target is at an altitude of 500 feet directly above the midpoint of a straight line connecting P and Q.

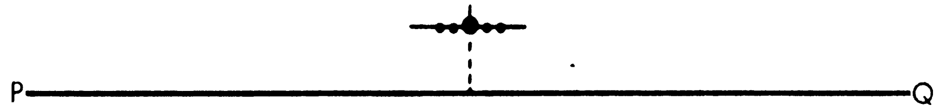

FIG. B-7 BASIC GEOMETRY USED IN THE DETERMINATION OF THE BISTATIC CROSS-SECTION OF THE TU-4 (B-29)

The monostatic case analyzed is the case in which the transmitter and receiver are both at Point P in Figure B-7. The monostatic radar cross-section was found to be 316 square meters.

The bistatic case analyzed is the case in which the transmitter is at P and the receiver at Q. The bistatic radar cross-section was found to be 55,300 square meters.

It might be well to point out that to date there is, to the authors' knowledge, neither experimental bistatic cross-section data on a B-29 for comparison, nor a method of obtaining an exact solution to the bistatic radar cross-section problem for objects of this complexity.

Although the value of 55,300 m^2 may seem large, it should be noted that Canadian early warning radar experiments indicate that large increases in radar cross-sections do result from bistatic operation.

B.3.2: The IL-28 (Type -27)

The radar characteristics of the IL-28 are based upon configurations appearing in Ref. B-6. Since small changes in the configuration of a scattering surface may produce significant changes in the scattered energy distribution, it is reasonable to expect that the following values of radar cross-section for the various aspects may change as more detailed information becomes available regarding the configuration. The IL-28 results are collected in Table B-2.*

Subsequent to the calculation of the radar cross-section for the IL-28, it was pointed out in Reference B-6 that a Russian IL-28 (Type 27) has approximately the same reflection characteristics as a B-45. Consequently, the theoretical values of radar cross-section for the IL-28 and the experimental values for the B-45 should be of the same order of magnitude. This is found to be the case, as illustrated in the following graphs. The type of comparison and the method of presentation are the same as in Figures B-8 to B-12.

*The meaning of the aspect angles θ and ϕ is indicated in Figure B-2.

ASPECT (in degrees)		RADAR CROSS-SECTION IN m^2		
θ	ϕ	X-Band	S-Band	L-Band
0	0	24.1	29.6	22.4
4	0	24.1	29.6	22.4
0	30	0.58	0.58	0.58
4	30	0.58	0.58	0.58
0	60	4.39	4.39	4.39
4	60	4.39	4.39	4.39
0	90	21000.	2090.	418.
4	90	1030.	453.	324.
0	120	4.36	4.36	4.36
4	120	4.36	4.36	4.36
0	150	0.38	0.38	0.38
4	150	0.38	0.38	0.38
0	180	0.38	0.38	0.38
4	180	0.38	0.38	0.38

σ for the IL-28

Table B-2

B.3.3: The MX-2091 and the 286-12 Bombers

The radar cross-sections of the MX-2091 and the 286-12 (see Fig's. B-13 and B-14) bombers have also been computed by these approximation techniques. The aspect angles shown in Figure B-2 were used.

The results obtained for the 286-12 are given in Tables B-3, B-4, and B-5. The results obtained for the MX-2091 are in Tables B-6, B-7, and B-8.

B.3.4: The B-47A

The theoretical physical-optics nose-on radar cross-section for the B-47A has been computed and previously reported in Reference B-7. The results obtained were as follows:

(1) L-Band, $\sigma = 2.79$ m^2
(2) S-Band, $\sigma = 7.44$ m^2

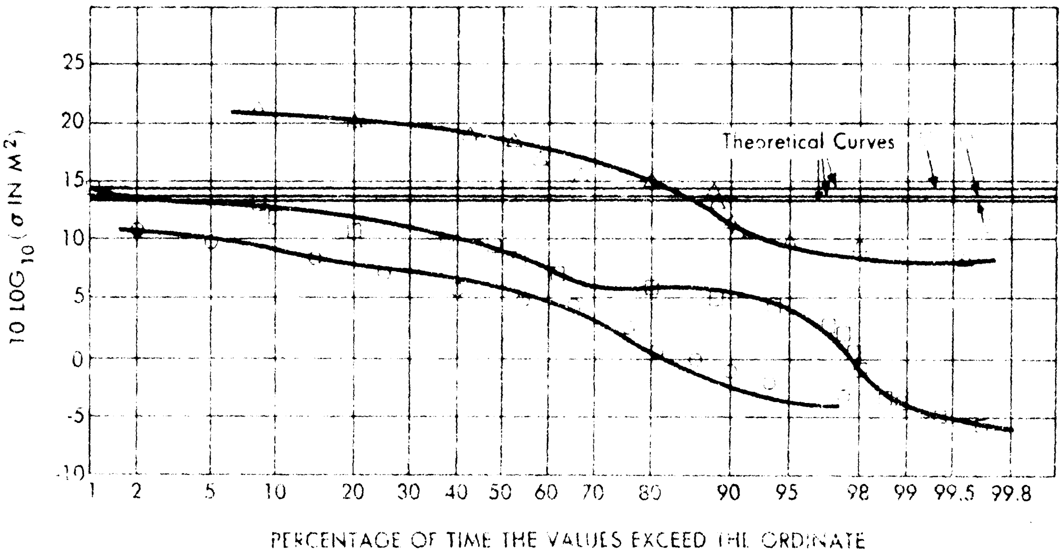

- 1250 Mc/sec.
- 2810 Mc/sec.
- 9380 Mc/sec.

FIG. B-8 COMPARISON OF THEORETICAL IL-28 CROSS-SECTION AND EXPERIMENTAL B-45 CROSS-SECTION AT ASPECT DEFINED BY AZIMUTH $\approx 0°$ AND ELEVATION $\approx 4°$

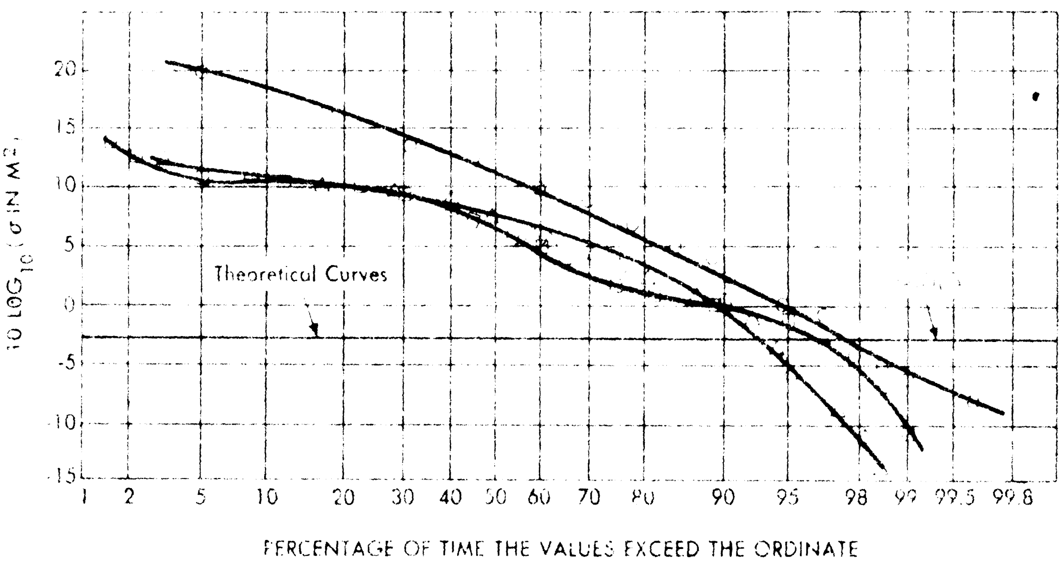

- 1250 Mc/sec.
- 2810 Mc/sec.
- 9380 Mc/sec.

FIG. B-9 COMPARISON OF THEORETICAL IL-28 CROSS-SECTION AND EXPERIMENTAL B-45 CROSS-SECTION AT ASPECT DEFINED BY AZIMUTH $\approx 30°$ AND ELEVATION $\approx 4°$

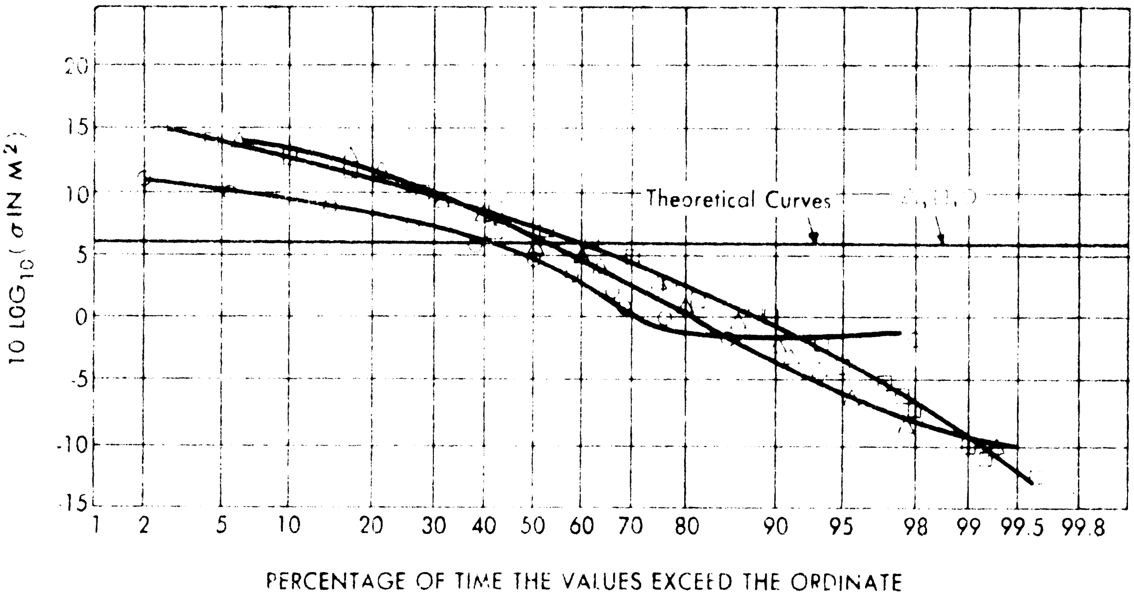

- 1250 Mc/sec.
- 2810 Mc/sec.
- 9380 Mc/sec.

FIG. B-10 COMPARISON OF THEORETICAL IL-28 CROSS-SECTION AND EXPERIMENTAL B-45 CROSS-SECTION AT ASPECT DEFINED BY AZIMUTH $\approx 60°$ AND ELEVATION $\approx 4°$

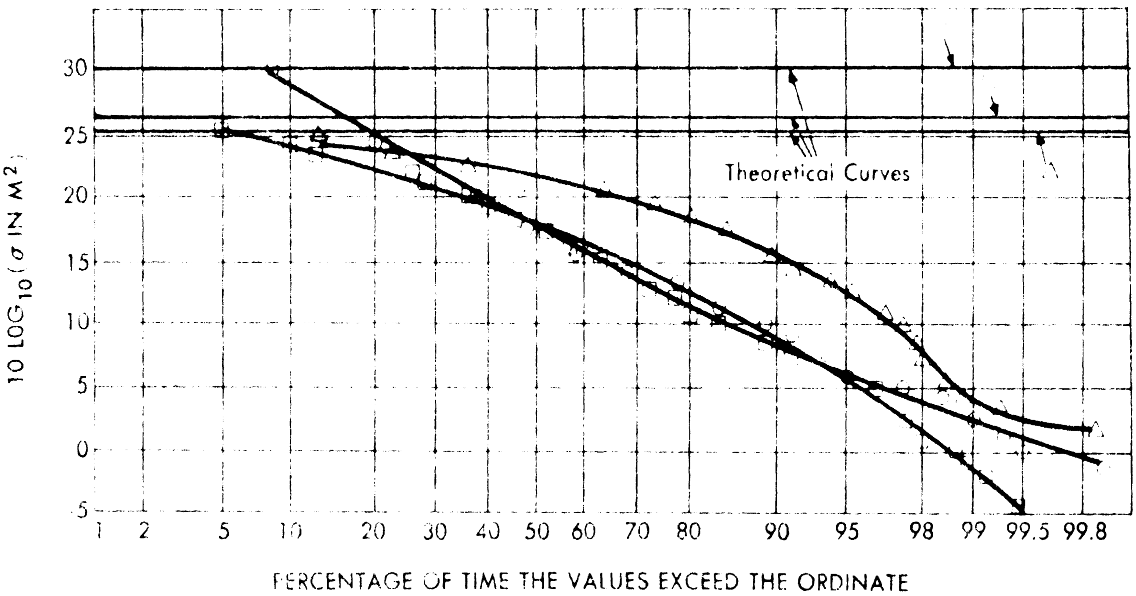

- 1250 Mc/sec.
- 2810 Mc/sec.
- 9380 Mc/sec.

FIG. B-11 COMPARISON OF THEORETICAL IL-28 CROSS-SECTION AND EXPERIMENTAL B-45 CROSS-SECTION AT ASPECT DEFINED BY AZIMUTH $\approx 90°$ AND ELEVATION $\approx 4°$

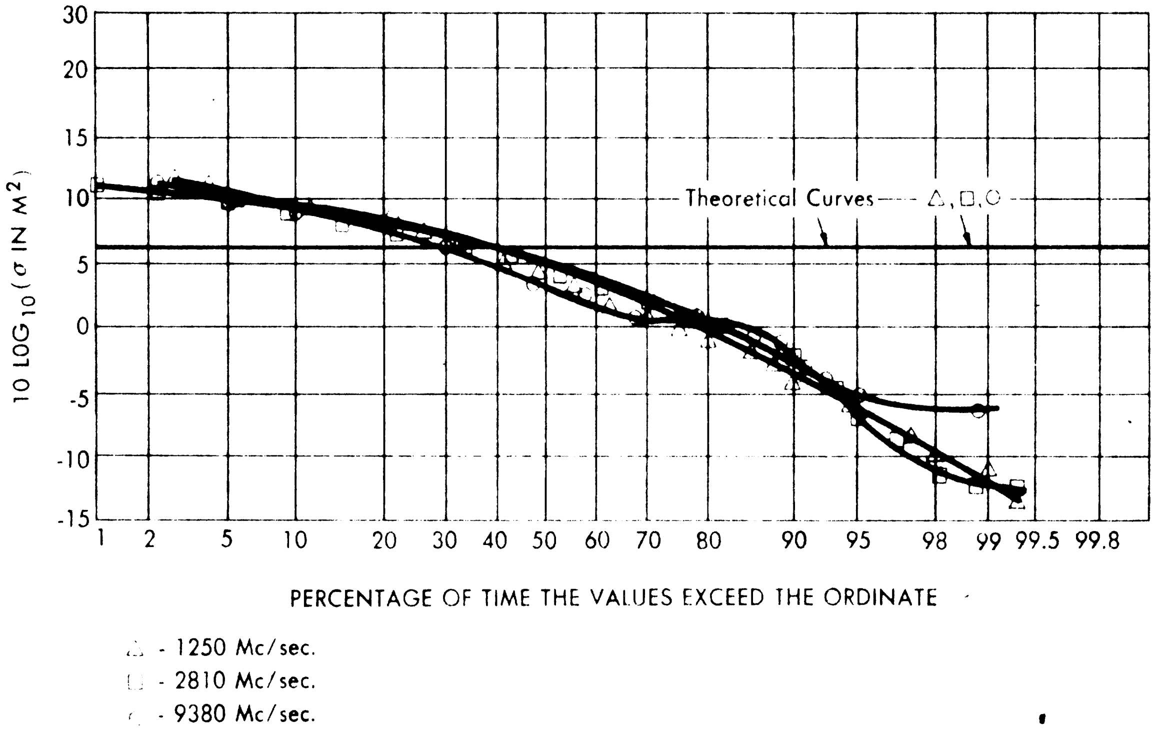

FIG. B-12 COMPARISON OF THEORETICAL IL-28 CROSS-SECTION AND EXPERIMENTAL B-45 CROSS-SECTION AT ASPECT DEFINED BY AZIMUTH ≈120° AND ELEVATION ≈4°

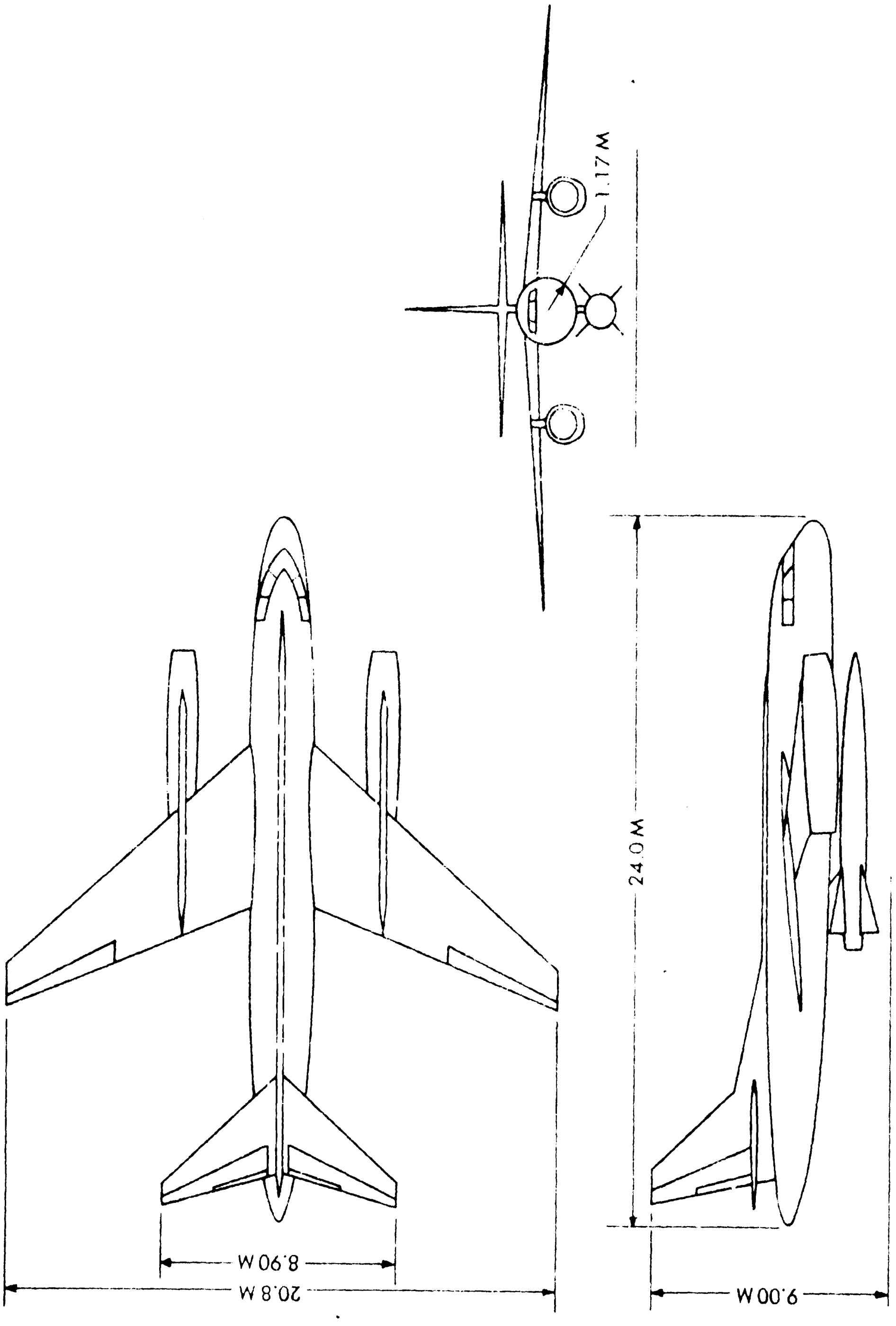

FIG. B-13 THE MX-2091

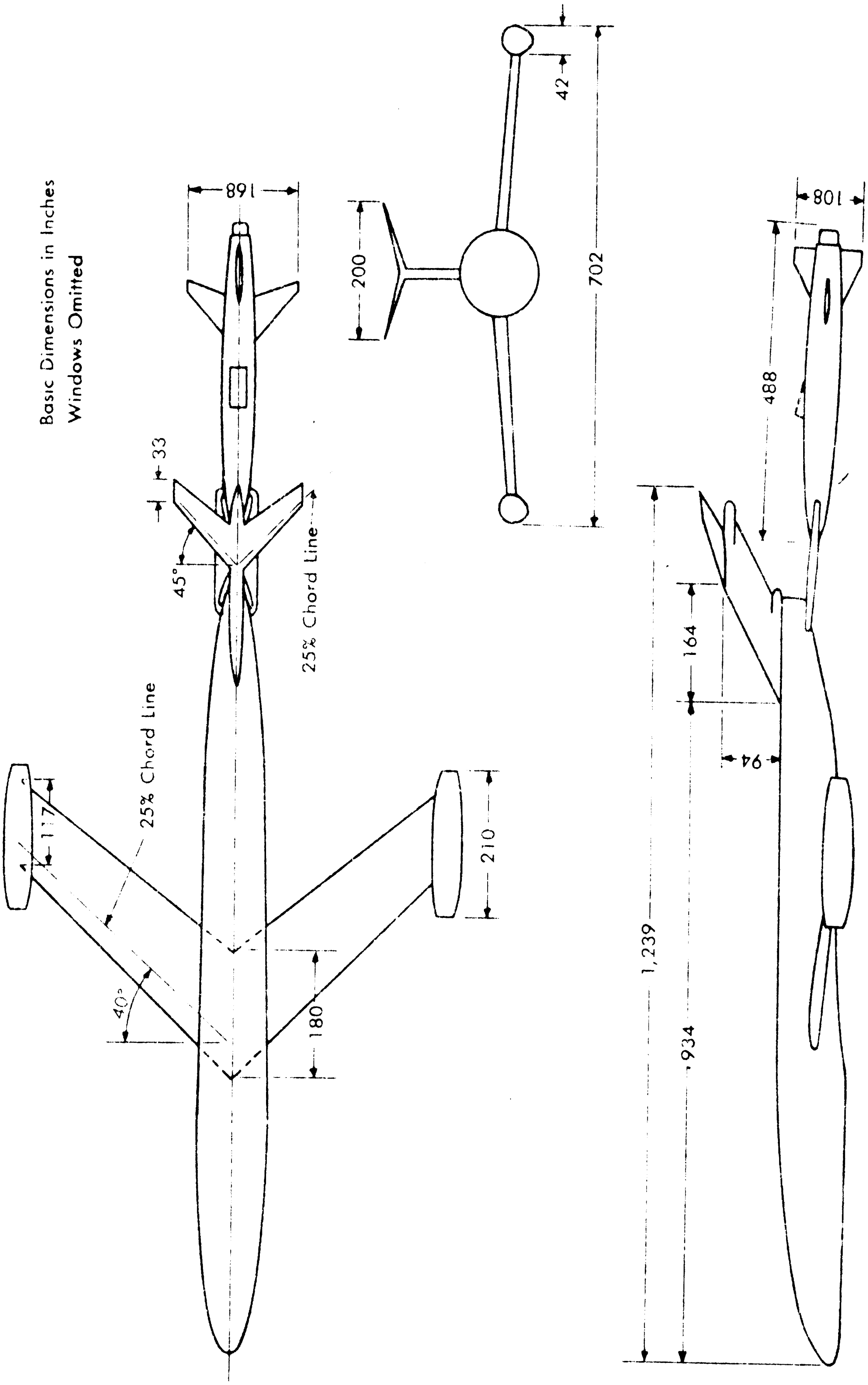

FIG. B-14 THE MARTIN 286-12

TABLE B-3

RADAR CROSS-SECTION OF THE 286-12 IN SQUARE METERS
(Without the Bomb)

ASPECT (in degrees)		WAVELENGTHS (in meters)		
ϕ	θ	λ = 0.03	λ = 0.10	λ = 0.25
0	0	87.	26.	19.
0	4	4.6	1.5	1.3
15	0	.35	.36	.37
15	4	.35	.36	.37
30	0	.53	.55	.60
30	4	.53	.56	.62
45	0	1.1	1.9	2.1
45	4	1.1	1.4	2.1
60	0	3.1	3.3	3.3
60	4	3.1	3.2	3.2
75	0	19.	17.0	20.
75	4	19.	16.	19.
85	0	48.	53.	49.
85	4	48.	51.	53.
90	0	31000	9400.	4300.
90	4	12000.	3700.	1600.
95	0	49.	53.	49.
95	4	47.	50.	120.
105	0	19.	20.	21.
105	4	19.	19.	20.
120	0	3.1	3.3	3.3
120	4	3.2	3.3	3.3
135	0	1.1	1.4	2.0
135	4	1.1	1.4	2.0
150	0	.53	.55	.60
150	4	.53	.55	.60
165	0	.35	.36	.37
165	4	.35	.36	.37
180	0	3.6	1.2	.70
180	4	.98	.50	.39

TABLE B-4

RADAR CROSS-SECTION OF THE 286-12 BOMB IN SQUARE METERS

ASPECT (in degrees)		WAVELENGTHS (in meters)		
ϕ	θ	$\lambda = 0.03$	$\lambda = 0.10$	$\lambda = 0.25$
0	0	$5.6 \cdot 10^{-6}$	$29.0 \cdot 10^{-6}$	$11.0 \cdot 10^{-4}$
0	4	$5.9 \cdot 10^{-6}$	$11.0 \cdot 10^{-6}$	$2.0 \cdot 10^{-5}$
15	0	.018	.018	.018
15	4	.019	.021	.026
30	0	.084	.083	.086
30	4	.086	.091	.10
45	0	.25	.27	.29
45	4	.25	.27	.29
60	0	.72	.76	.83
60	4	.72	.76	.83
75	0	3.5	3.7	4.
75	4	3.5	3.7	4.
85	0	92.	93.	96.
85	4	92.	93.	96.
90	0	15000.	1600.	240.
90	4	1200.	630.	470.
95	0	32.	33.	35.
95	4	32.	33.	35.
105	0	3.5	3.7	3.9
105	4	3.5	3.7	3.9
120	0	.72	.76	.81
120	4	.72	.76	.81
135	0	.25	.27	.29
135	4	.25	.27	.29
150	0	.085	.091	.10
150	4	.085	.091	.10
165	0	.019	.021	.026
165	4	019	.021	.026
180	0	2.1	.67	.32
180	4	.33	.096	.079

TABLE B-5

RADAR CROSS-SECTION OF THE 286-12 AND BOMB
IN SQUARE METERS

ASPECT (in degrees)		WAVELENGTHS (in meters)		
ϕ	θ	λ = 0.03	λ = 0.10	λ = 0.25
0	0	87.	26.	1.9
0	4	4.6	1.5	1.5
15	0	.37	.37	.39
15	4	.37	.38	.39
30	0	.61	.63	.69
30	4	.62	.65	.73
45	0	1.3	2.2	2.4
45	4	1.3	1.7	2.4
60	0	3.9	4.0	4.1
60	4	3.9	4.0	4.0
75	0	22.	20.	24.
75	4	23.	20.	23.
85	0	140.	150.	140.
85	4	140.	140.	150.
90	0	46000.	11000.	4500.
90	4	13000.	43000.	2100.
95	0	80.	92.	84.
95	4	78.	83.	150.
105	0	22.	23.	25.
105	4	22.	23.	24.
120	0	3.9	4.0	4.1
120	4	3.9	4.0	4.1
135	0	1.3	1.7	2.3
135	4	1.3	1.7	2.3
150	0	.62	.64	.70
150	4	.62	.64	.70
165	0	.37	.38	.39
165	4	.37	.38	.39
180	0	5.7	1.9	.73
180	4	1.3	.60	.47

TABLE B-6

RADAR CROSS-SECTION OF THE MX-2091 IN SQUARE METERS
(Without the Bomb)

ASPECT (in degrees)		WAVELENGTHS (in meters)		
ϕ	θ	$\lambda = 0.03$	$\lambda = 0.10$	$\lambda = 0.25$
0	0	.37	.37	.38
0	4	.37	.37	.38
15	0	.02	.02	.02
15	4	.02	.02	.03
30	0	.08	.09	.13
30	4	.08	.14	.19
45	0	.20	.22	.29
45	4	.15	.18	.32
60	0	.80	.92	.12
60	4	.58	.59	1.7
75	0	6.8	8.0	12.
75	4	6.4	6.6	12.
85	0	160.	250.	340.
85	4	160.	190.	250.
90	0	27000.	8300.	3400.
90	4	520.	600.	690.
95	0	160.	250.	350.
95	4	1000.	2100.	1000.
105	0	6.2	7.4	12.0
105	4	6.3	8.3	9.0
120	0	.90	1.1	1.4
120	4	.86	.91	1.3
135	0	.31	.34	.37
135	4	.31	.33	.40
150	0	.02	.03	.10
150	4	.02	.03	.09
165	0	.06	.39	3.2
165	4	.03	.05	.19
180	0	6.3	1.9	.88
180	4	31.	9.4	.39

TABLE B-7

RADAR CROSS-SECTION OF THE MX-2091 BOMB
IN SQUARE METERS

ASPECT (in degrees)		WAVELENGTHS (in meters)		
ϕ	θ	λ = 0.03	λ = 0.10	λ = 0.25
0	0	$6.7 \cdot 10^{-7}$	$7.2 \cdot 10^{-7}$	$2.2 \cdot 10^{-5}$
0	4	$5.9 \cdot 10^{-7}$	$3.2 \cdot 10^{-5}$	$2.8 \cdot 10^{-4}$
15	0	.0074	.0074	.0074
15	4	.0074	.0074	.0075
30	0	.035	.035	.035
30	4	.035	.035	.035
45	0	.10	.10	.10
45	4	.10	.10	.10
60	0	.31	.31	.31
60	4	.31	.31	.31
75	0	1.7	1.6	1.5
75	4	1.7	1.6	1.5
85	0	130.	150.	150.
85	4	120.	130.	150.
90	0	59000.	5700.	1000.
90	4	1000.	1000.	1000.
95	0	120.	120.	120.
95	4	120.	120.	120.
105	0	1.5	1.4	1.4
105	4	1.5	1.4	1.4
120	0	.31	.31	.31
120	4	.31	.31	.31
135	0	.10	.10	.10
135	4	.10	.10	.10
150	0	.035	.035	.035
150	4	.035	.035	.036
165	0	.0076	.0082	.0075
165	4	.0076	.0081	.0079
180	0	1.5	.52	.26
180	4	.69	.30	.17

TABLE B-8

RADAR CROSS-SECTION OF MX-2091 AND BOMB
IN SQUARE METERS

ASPECT (in degrees)		WAVELENGTHS (in meters)		
ϕ	θ	$\lambda = 0.03$	$\lambda = 0.10$	$\lambda = 0.25$
0	0	.37	.37	.38
0	4	.37	.37	.38
15	0	.023	.028	.25
15	4	.023	.025	.034
30	0	.12	.12	.16
30	4	.12	.17	.26
45	0	.30	.32	.40
45	4	.26	.29	.42
60	0	1.1	1.2	1.5
60	4	.89	.90	2.0
75	0	8.5	9.6	13.
75	4	8.1	14.	13.
85	0	290.	400.	540.
85	4	290.	320.	400.
90	0	86000.	14000.	4500.
90	4	1500.	1600.	1700.
95	0	280.	380.	470.
95	4	1200.	2200.	1200.
105	0	7.6	8.8	13.
105	4	7.7	9.7	10.
120	0	1.2	1.4	1.7
120	4	1.2	1.2	1.6
135	0	.42	.45	.47
135	4	.42	.43	.50
150	0	.059	.065	.13
150	4	.057	.069	.13
165	0	.066	.40	3.2
165	4	.038	.057	.20
180	0	34.	2.6	1.3
180	4	42.	13.	4.3

B.4: The Cross-Section of Missiles

Using the aspect connotation given in Figure B-2, where the θ and ϕ aspect angles are defined, and employing the techniques briefly outlined in Section B.2, the radar cross-section of the Loon, Regulus, and Snark Missiles were determined at various aspects and at the three frequencies denoted by X-band, S-band, and L-band. The configurations used were taken from References B-8, B-9, and B-10 respectively and the results of the computations are given in Tables B-9, 10, and 11.

Other missiles have been considered but not in as great detail as those we have previously mentioned. All other theoretical missile cross-section determinations made at the Willow Run Research Center are listed in Table B-12, except ballistic missiles which will be analyzed separately in a future publication in this series.

ASPECT (in degrees)		RADAR CROSS-SECTION IN m^2		
θ	ϕ	X-Band	S-Band	L-Band
0	0	37.8	12.6	5.4
4	0	37.8	12.6	5.4
0	30	0.23	0.30	0.23
4	30	0.23	0.30	0.23
0	60	1.55	1.51	1.51
4	60	1.55	1.51	1.51
0	80	16.5	16.5	17.1
4	80	16.5	16.5	17.1
0	85	28.2	28.2	28.2
4	85	28.2	28.2	28.2
0	90	664.	227.	83.0
4	90	283.	143.	148.
0	100	21.6	21.6	22 1
4	100	21.6	21.6	22.1
0	105	34.8	34.8	35.4
4	105	34.8	34.8	35.4
0	120	2.63	2.63	2.58
4	120	2.63	2.63	2.58
0	150	0.45	0.52	0.45
4	150	0.45	0.52	0.45
0	180	4.11	2.02	1.15
4	180	4.11	2.02	1.15

σ for the Loon Missile

Table B-9

ASPECT (in degrees)		RADAR CROSS-SECTION IN m^2		
θ	ϕ	X-Band	S-Band	L-Band
0	0	21.7	6.5	2.6
4	0	21.7	6.5	2.6
0	30	.060	.060	.060
4	30	.060	.060	.060
0	60	0.486	0.486	0.486
4	60	0.486	0.486	0.486
0	90	4680.	1480.	640.
4	90	98.	150.	259.
0	120	0.486	0.486	0.486
4	120	0.486	0.486	0.486
0	150	.060	.060	.060
4	150	.060	.060	.060
0	180	745.	66.8	10.7
4	180	745.	66.8	10.7

σ for the Regulus Missile

Table B-10

ASPECT (in degrees)		RADAR CROSS-SECTION IN m^2		
θ	ϕ	X-Band	S-Band	L-Band
0	0	0.13	0.13	0.13
4	0	0.13	0.13	0.13
0	30	0.21	0.22	0.22
4	30	0.21	0.22	0.22
0	60	1.51	1.54	1.59
4	60	1.51	1.54	1.59
0	80	13.4	13.58	14.08
4	80	13.4	13.58	14.08
0	85	19.4	19.6	19.83
4	85	19.4	19.6	19.83
0	90	14900.	4500.	1847.
4	90	14900.	4500.	1847.
0	95	19.4	19.6	19.83
4	95	19.4	19.6	19.83
0	100	13.4	13.58	14.08
4	100	13.4	13.58	14.08
0	120	1.51	1.54	1.59
4	120	1.51	1.54	1.59
0	150	0.21	0.22	0.22
4	150	0.21	0.22	0.22
0	180	1020.	91.8	14.7
4	180	8.87	8.87	8.87

σ for the Snark Missile

Table B-11

MISSILE	ASPECT	WAVE LENGTH	σ IN m^2	REFERENCE FOR CONFIGURATION DATA
Navaho	Nose-on	λ = 1ft.	.8	B-11
Rascal	Nose-on	λ = 1ft.	.12	B-12
Big Richard	Nose-on	λ = 1ft.	.67	B-13
G-2	Nose-on	λ = 1ft.	.60	B-13
Bomarc	Nose-on	λ = 1ft.	.16	B-14
Bomarc	30° off nose-on	λ = 1ft.	.11	B-14
Bomarc	60° off nose-on	λ = 1ft.	.98	B-14
Bomarc	80° off nose-on	λ = 1ft.	2.38	B-14
Bomarc	Broadside	λ = 1ft.	1300.	B-14
Bomarc	100° off nose-on	λ = 1ft.	2.2	B-14
Bomarc	120° off nose-on	λ = 1ft.	94	B-14
Bomarc	150° off nose-on	λ = 1ft.	.12	B-14
Bomarc	Tail-on	λ = 1ft.	14.2	B-14
Lockheed Ramjet (missile only)	Nose-on	X-band	.04	B-15
"	Nose-on	S-band	.057	B-15
"	Nose-on	L-band	.17	B-15
Lockheed Ramjet (missile + jetbrace)	Nose-on	X-band	.04	B-15
"	Nose-on	S-band	.057	B-15
"	Nose-on	L-band	.17	B-15
Lockheed Ramjet (missile + jet)	Nose-on	X-band	.062	B-15
"	Nose-on	S-band	.069	B-15
"	Nose-on	L-band	.193	B-15
"	Broadside	X-band	$2000 < \sigma < 12300$	B-15
"	Broadside	S-band	$600 < \sigma < 1500$	B-15
"	Broadside	L-band	$200 < \sigma < 310$	B-15
Redstone Missile	Nose-on	-	.18	-
Nike	Nose-on	-	.07	-
Matador	Nose-on	-	.22	-

σ for Other Missiles

Table B-12

MISSING
PAGE

B9 XSSM-N-8 Regulus Progress Report #1 (covering review of progress through June 1951), Chance Vought Aircraft, Dallas, Texas. SECRET.

B10 Project Snark, (A review intended to supplement lecture material scheduled for presentation for the USAF Institute of Technology Guided Missile Seminar & Wright Patterson AFB, May 1951), Northrup Aircraft, Hawthorne, California. SECRET.

B11 "Standard Missile Characteristics", WADC Report.

B12 "Bell Aircraft Quarterly Progress Report - Project Rascal - Project Shrike, BMPR-25, June 1951. SECRET.

B13 "Surface to Surface Guided Missiles", Air Technical Intelligence Center, Study No. 120-AC-51/44-34, January 1952. SECRET.

B14 "Bomarc Missile Design Data", Boeing Airplane Company, Document D-11550, Model MX1599, September 1951. SECRET.

B15 Jenks, F. P. and Thoren, R. L., "Ram Jet Test Vehicle Report", Lockheed Aircraft Corporation, Progress Report No. 22, October 1951. CONFIDENTIAL.

APPENDIX C

EXACT SOLUTION TO ELECTROMAGNETIC SCATTERING PROBLEMS

Exact solutions of Maxwell's equations for boundary value problems involving the scattering of electromagnetic waves by three-dimensional configurations are very few indeed. The few exact solutions which are known are discussed below.

The Sphere

The cross-section of a sphere was determined theoretically by Mie (Ref. C-1), Stratton (Ref. C-2), Kerr (Ref. C-3), Aden (Ref. C-4), Ohio State University (Ref. C-5), University of California (Ref. C-6), and Brillouin (Ref. C-7). The above papers involved spheres which are perfect conductors (Ref. C-1, 2, 3, 5, 6, 7) and also dielectric spheres (Ref. C-1, 2, 3, 4).

Only in references C-5 and C-6 is found a comparison between theory and experiment for conducting spheres of a particular size, where the transmitter and the receiver are separated. Only reference C-4 compares theory and experiment for water spheres.

Thus it is apparent that there is much to be done both theoretically and experimentally before the general electromagnetic scattering from even such a simple shape as a sphere is generally understood. The theoretical aspect involves such matters as summability techniques and the task of computing many more numerical values of cross-section. A parallel expansion of experimental data pertaining to the dielectric sphere is necessary for an evaluation of the theoretical results.

The Prolate Spheroid

The back-scattering cross-section of a conducting prolate spheroid has been determined exactly by Schultz when the incident Poynting Vector is on the axis of symmetry (Ref. C-8). Some of his results have been used in the computation of the prolate spheroid's cross-section by the

Willow Run Research Center on the Mark III and his theoretical results have been extended to general receiver location in Reference C-9. Reference C-9 also solves several of the theoretical questions involving the prolate spheroidal recursion formulas.

No experimental results have been published, to our knowledge, although some experimental work on the prolate spheroid is being conducted at the University of California under Prof. S. Silver.

Again there is still much numerical as well as theoretical work to be done, especially in the dielectric case, which is practically untouched, as well as in the general bistatic case.

The Cone

The work of Hansen and Schiff (Ref. C-10) and Willow Run Research Center (Refs. C-11 & C-12) has resulted in the exact cross-section for axially symmetric back-scattering from a semi-infinite conducting cone. It is shown that up to at least a second order approximation for both small and large cone angles the exact result is in agreement with the physical optics result

$$\sigma = \frac{\lambda^2 \tan^4 \theta}{16\pi}$$

where σ is the cross-section, λ is the wavelength, and θ is 1/2 the cone angle.

Sletten (Ref. C-13) has done the experimental work for the axially symmetric back-scattering problem. Work has been started on other theoretical cone problems and it is believed that before too long a time the conducting cone problem will have been completely resolved.

To our knowledge no work, either experimental or theoretical, has been conducted concerning the dielectric cone.

The Oblate Spheroid

In the ninth paper in the series of studies on scattering cross-sections, the exact solution of the radar cross-section of an oblate spheroid was obtained by the method due to Hansen (Ref. C-14). The solution obtained was for the case in which the transmitter and receiver were both situated along the axis of symmetry for a perfectly conducting spheroid. As in the case of the sphere, for example, the radar cross-section has been obtained in the form of an infinite series.

Unfortunately the defining relations for the coefficients in the series are quite complex and their values have not been tabulated very extensively. Consequently no numerical values of radar cross-sections exist as yet for the oblate spheroid.

The Paraboloid

A solution has been obtained at the Willow Run Research Center for a semi-infinite paraboloid. It has been found (Ref. C-15) for the case in which the transmitter is along the axis of symmetry of the paraboloid that the exact radar cross-section can be obtained by the Luneberg-Kline method, based upon geometrical optics considerations. The exact bistatic radar cross-section of a paraboloid is plotted in Figure C-1. One can observe by substituting directly into Maxwell's equations and the boundary conditions that the geometric optics solution for the above case is the exact solution.

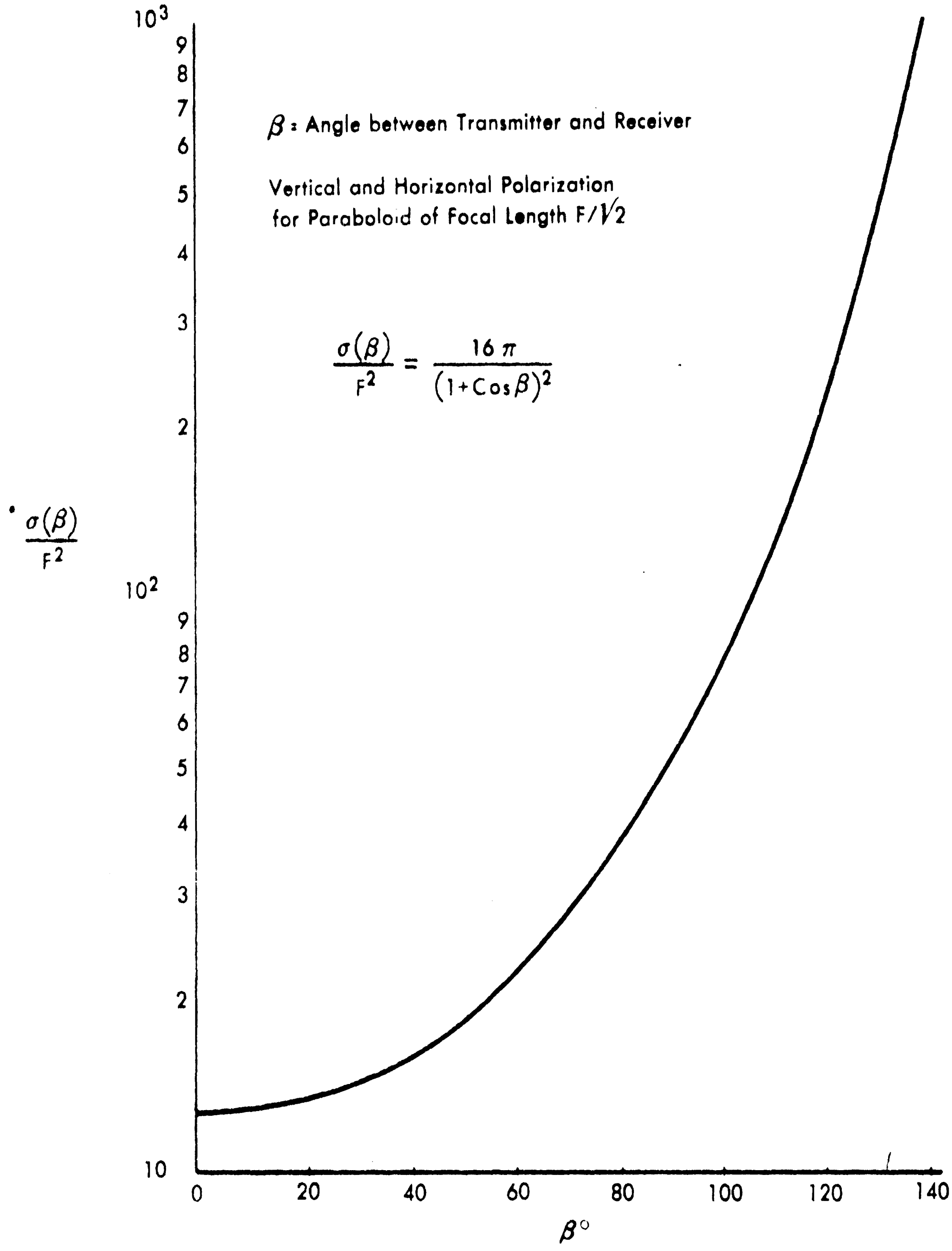

FIG. C-1 CROSS-SECTION OF A PARABOLOID AS A FUNCTION OF β

REFERENCES

FOR APPENDIX C

C1 Mie, G., "Beitraege zur Optik trueber Medien, speziell Kolloidaler Metalloesungen," Annalen der Physik, vol. 25, p. 377, 1908.

C2 Stratton, J. A., Electromagnetic Theory, McGraw-Hill Book Co., New York, 1941.

C3 Kerr, D. E., Propagation of Short Radio Waves, McGraw-Hill Book Co., New York, 1951.

C4 Aden, A. L., "Electromagnetic Scattering From Metal and Water Spheres", Harvard University, Cruft Laboratory, Technical Report No. 106, (ATI-92016), August 1950. UNCLASSIFIED.

C5 "Echoing Area Characteristics of Various Objects: Ninth Quarterly Progress Report," Ohio State University Research Foundation, Report-302-29, May 1949. CONFIDENTIAL.

C6 Hamren, S. D., "Scattering from Spheres," University of California, Antenna Laboratory, Report No. 171, (ATI-83900), June 1950. UNCLASSIFIED.

C7 Brillouin, L., "On Light Scattering by Spheres II," Columbia University, Applied Mathematics Panel, Report Columbia AMP-87-2, (OSRD-3464), April 1944. UNCLASSIFIED.

C8 Schultz, F. V., "Studies in Radar Cross-Sections I, Scattering by a Prolate Spheroid," Willow Run Research Center, University of Michigan, Report UMM-42, March 1950. UNCLASSIFIED.

C9 Siegel, K. M., Gere, B. H., Marx, I., Sleator, F. B., "Studies in Radar Cross-Sections XI, The Numerical Determination of the Radar Cross-Section of a Prolate Spheroid," Willow Run Research Center, University of Michigan, Report UMM-126, December 1953. UNCLASSIFIED.

C10 Hansen, W. W., Schiff, L. I., "Theoretical Study of Electromagnetic Waves Scattered From Shaped Metal Surfaces," Quarterly Report No. 4, Stanford University, Microwave Laboratory, ATI-46568, September 1948. UNCLASSIFIED.

C11 Siegel, K. M., Alperin, H. A., "Studies in Radar Cross-Sections III, Scattering by a Cone," Willow Run Research Center, University of Michigan, Report No. UMM-87, January 1952. UNCLASSIFIED.

C12 Siegel, K. M., Alperin, H. A., Crispin, J. W., Hunter, H. E., Kleinman, R. E., Orthwein, W. C., Schensted, C. E., "Studies in Radar Cross-Section-IV, Comparison Between Theory and Experiment of the Cross-Section of a Cone," Willow Run Research Center, University of Michigan, Report No. UMM-92, February 1953. UNCLASSIFIED.

C13 Sletten, C. J., "Electromagnetic Scattering From Wedges and Cones," Cambridge Research Center, Report CRC-E5090, July 1952. UNCLASSIFIED.

C14 Hansen, W. W., "A New Type of Expansion in Radiation Problems," The Physical Review, vol. 47, January 15, 1935.

C15 Siegel, K. M., Alperin, H. A., Bonkowski, R. R., Crispin, J. W., Maffett, A. L., Schensted, C. E., Schensted, I. V., "Studies in Radar Cross-Sections VIII, Theoretical Cross-Section as a Function of Separation Angle Between Transmitter and Receiver at Small Wavelengths," Willow Run Research Center, University of Michigan, Report No. UMM-115, October 1953. UNCLASSIFIED.

DISTRIBUTION

To be distributed in accordance with the Terms of the Contract.